



**UNIVERDIDADE FEDERAL DA FRONTEIRA SUL
CAMPUS LARANJEIRAS DO SUL
PROGRAMA DE PÓS-GRADUAÇÃO EM CIÊNCIA E TECNOLOGIA DE ALIMENTOS**

RUBIA VIANA BATISTA

**MODELAGEM MATEMÁTICA E SIMULAÇÃO NUMÉRICA DO TRANSPORTE DE
OXIGÊNIO EM FILME MULTICAMADAS PARA USO EM ALIMENTOS:**

UMA ABORDAGEM SEMI-ANALÍTICA

LARANJEIRAS DO SUL

2020

RUBIA VIANA BATISTA

**MODELAGEM MATEMÁTICA E SIMULAÇÃO NUMÉRICA DO TRANSPORTE DE
OXIGÊNIO EM FILME MULTICAMADAS PARA USO EM ALIMENTOS:**

UMA ABORDAGEM SEMI-ANALÍTICA

Dissertação apresentada ao Programa de Pós-graduação em Ciência e Tecnologia de Alimentos, Universidade Federal da Fronteira Sul como requisito parcial para obtenção do título de Mestre em Ciência e Tecnologia de Alimentos.

Orientadora: Prof.^a Dr.^a Vivian Machado de Menezes

Coorientador: Prof. Dr. Wanderson Gonçalves Wanzeller

LARANJEIRAS DO SUL

2020

Bibliotecas da Universidade Federal da Fronteira Sul - UFFS

Batista, Rubia Viana

Modelagem matemática e simulação numérica do
transporte de oxigênio em filme multicamadas para uso em
alimentos: uma abordagem semi-analítica. / Rubia Viana
Batista. -- 2020.

59 f.:il.

Orientadora: Profª. Drª. Vivian Machado de Menezes

Co-orientador: Prof. Dr. Wanderson Gonçalves

Wanzeller

Dissertação (Mestrado) - Universidade Federal da
Fronteira Sul, Programa de Pós-Graduação em Ciência e
Tecnologia de Alimentos, Laranjeiras do Sul, PR, 2020.

1. Métodos numéricos. 2. Difusão de gases. 3. Filmes
poliméricos. 4. Embalagem de alimentos. 5. Sistemas
multicamadas. I. Menezes, Vivian Machado de, orient. II.
Wanzeller, Wanderson Gonçalves, co-orient. III.
Universidade Federal da Fronteira Sul. IV. Título.

RUBIA VIANA BATISTA

**MODELAGEM MATEMÁTICA E SIMULAÇÃO NUMÉRICA DO TRANSPORTE DE
OXIGÊNIO EM FILME MULTICAMADAS PARA USO EM ALIMENTOS:
UMA ABORDAGEM SEMI-ANALÍTICA.**

Dissertação apresentada ao Curso de Pós-graduação *Stricto sensu*, da Universidade Federal da Fronteira Sul – UFFS, para obtenção do título de Mestra em Ciência e Tecnologia de Alimentos.

Este trabalho de conclusão de curso foi defendido e aprovado pela banca em:

05/10/2020

BANCA EXAMINADORA¹

Prof.^a Dra. Vivian Machado de Menezes (UFFS – presidente/orientadora)

Prof. Dr. Wanderson Gonçalves Wanzellier (UFFS – coorientador)

Prof. Dr. Gustavo Henrique Fidelis dos Santos (UFFS – 1º membro)

Prof. Dr. Carlos Augusto Fernandes Dagnone (UFFS – 2º membro)

Prof.^a Dra. Vânia Zanella Pinto (UFFS – suplente)

¹"Em função da Pandemia do Coronavírus e as medidas de ajustamento tomadas pela UFFS, esta Folha de Aprovação foi assinada pelo Presidente da Banca, como representante dos demais membros".

DEDICATÓRIA

Dedico a meus pais, meu irmão e meu esposo, os quais sempre me apoiaram e foram meu refúgio durante esta etapa de minha vida. Amo vocês

AGRADECIMENTOS

A Deus pela vida, por todas as bençãos e força para enfrentar os obstáculos.

Ao meu querido esposo Eloibiso Schadeck de Siqueira, por todo amor, carinho, compreensão nos momentos de ausência e por sempre me apoiar nas minhas escolhas e não medir esforços para que eu pudesse concluir meu trabalho, por acreditar em mim mais que eu mesma. Amo você.

Aos meus pais, Terezinha Viana e Celso Marino Moreira Batista, meu irmão Fabio Viana Batista, por todo amor, palavras de carinho, conselhos, amizade e por sempre me apoiar e incentivar. Amo vocês incondicionalmente.

À minha orientadora Profª. Drª. Vivian Machado de Menezes por toda paciência, compreensão e dedicação para que o trabalho fosse desenvolvido, por todos os conhecimentos transmitidos. Gratidão por encontrar pessoas como você pelo caminho e pela amizade.

Ao meu coorientador Prof. Dr. Wanderson Gonçalves Wanzeller pela grande paciência, compreensão e não medir esforços para realização deste trabalho, por todo conhecimento compartilhado. Obrigada por além de professor também ser um amigo.

Aos professores Prof. Dr. Carlos Augusto Fernandes D'Agnone, Prof. Dr. Gustavo Henrique Fidelis dos Santos, Profª. Drª Vânia Zanella Pinto, por aceitarem compor a banca da minha defesa de dissertação, por todas as considerações e por dispor de seu tempo para contribuir com este trabalho.

Aos professores que me orientaram nos estágios docência, Prof. Dr. Ernesto Quast, Prof. Dr. Gustavo Henrique Fidelis dos Santos e Profª. Drª. Larissa Canhadas Bertan, por toda confiança e por todo auxílio e conselhos, para que eu pudesse vivenciar a experiência da docência.

Aos demais professores, Profª. Drª. Eduarda Molardi Bainy, Profª. Drª Vânia Zanella Pinto, Profª. Drª. Leda Basttestin Quast, que me orientaram e auxiliaram na elaboração de oficinas, cursos e palestras. E aos demais professores do Programa de Pós-graduação em Ciência e Tecnologia de Alimentos pela dedicação e por compartilhar seus conhecimentos.

A todos os amigos e colegas com quem pude compartilhar além das atividades acadêmicas, bons momentos de descontração ao longo desse período. Vocês fizeram essa caminhada mais leve.

EPÍGRAFE

“Tenho a impressão de ter sido uma criança brincando à beira-mar, divertindo-me em descobrir uma pedrinha mais lisa ou uma concha mais bonita que as outras, enquanto o imenso oceano da verdade continua misterioso diante de meus olhos”. (Isaac Newton)

APRESENTAÇÃO

Esta dissertação de mestrado está apresentada na forma de dois artigos científicos:

TEXTO PRINCIPAL: Batista, Rubia Viana; Wanzeller, Wanderson Gonçalves; Menezes, Vivian Machado de. 2020. Modelagem matemática e simulação numérica do transporte de oxigênio em filme multicamadas para uso em alimentos: uma abordagem semi-analítica. Submetido ao periódico científico AIChE Journal, an Official Publication of The American Institute of Chemical Engineers.

ANEXO: Batista, Rubia Viana; Wanzeller, Wanderson Gonçalves; Lim, Loong-Tak; Quast, Ernesto; Pinto, Vânia Zanella; Menezes, Vivian Machado de. 2020. Applications and oxygen transfer models in active multilayer food packing: a theoretical review. Será submetido ao periódico científico Trends in Food Science and Technology.

RESUMO

O objetivo do presente estudo foi desenvolver uma metodologia de simulação numérica capaz de prever o comportamento do oxigênio frente a sistemas poliméricos multicamadas, a fim de otimizar configurações de embalagem com maior barreira a esse gás. Foi utilizado o método da Transformada de Laplace para resolução das equações diferenciais parciais, com inversão numérica pelo algoritmo de Stehfest com o método de Gauss-Sidel, utilizando linguagem *Fortran 77* e um compilador livre. Com essa metodologia foi possível simular o perfil de concentração de oxigênio frente a sistemas de embalagem contendo dois ou três materiais na configuração (ABA ou ABC). Para alguns sistemas, aumentando o tempo de simulação, a função concentração apresentava flutuação numérica na interface dos materiais, principalmente se o oxigênio difundia de um material com difusividade maior para um com difusividade menor. Quanto maior a diferença entre a ordem de grandeza dos coeficientes de difusão, maior é a flutuação numérica encontrada. O perfil de concentração de oxigênio simulado numericamente pode ser associado a resultados da literatura, validados experimentalmente. Os resultados mostraram-se promissores para aplicação em problemas de difusão em sistemas multicamadas e a metodologia pode ser utilizada para descrever sistemas com maior número de camadas.

Palavras-chave: métodos numéricos; difusão de gases; filmes poliméricos; embalagem de alimentos, sistemas multicamadas.

ABSTRACT

The purpose of the present study was to develop a numerical simulation methodology capable of predicting the behavior of oxygen against multilayer polymeric systems, to optimize packaging configurations with a greater barrier to this gas. The Laplace Transform method was used to solve partial differential equations, with numerical inversion by the Stehfest algorithm with the Gauss-Sidel method, using Fortran 77 language and a free compiler. With this methodology, it was possible to simulate the oxygen concentration profile in front of packaging systems containing two or three materials in the configuration (ABA or ABC). For some systems, increasing the simulation time, the concentration function showed numerical fluctuation at the material interface, especially if oxygen diffused from a material with greater diffusivity to one with less diffusivity. The greater the difference between the order of magnitude of the diffusion coefficients, the greater the numerical fluctuation found. The numerically simulated oxygen concentration profile can be associated with results from the literature, experimentally validated. The results showed to be promising for application in diffusion problems in multilayer systems and the methodology can be used to describe systems with a greater number of layers.

Keywords: numerical methods; diffusion of gases; polymeric films; food packaging; multilayer systems.

LISTA DE FIGURAS

Figura 1 - Representação do filme multicamadas com configurações ABA (a) e ABC (b).

Figura 2 - Perfil de concentração do oxigênio no interior de filme multicamada composto por PE/EVOH/PE - configuração ABA. Elaborado com *Xmgrace*[®].

Figura 3 - Perfil de concentração do oxigênio no interior de filme multicamada composto por PP/EVOH/PP - configuração ABA. Elaborado com *Xmgrace*[®].

Figura 4 - Perfil de concentração do oxigênio no interior de filme multicamada composto por PET/EVOH/PET - configuração ABA. Elaborado com *Xmgrace*[®].

Figura 5 - Perfil de concentração do oxigênio no interior de filme multicamada composto por PET/PP/PET - configuração ABA. Elaborado com *Xmgrace*[®].

Figura 6 - Perfil de concentração do oxigênio no interior de filme multicamada composto por PET/EVOH/PE - configuração ABC. Elaborado com *Xmgrace*[®].

Figure A1 - Scheme of a spherical particle of an oxygen scavenging polymer (OSP) and particle reduction due to oxidation. C_P is the oxygen concentration in OSP particle. (Adapted from Ferrari et al., 2009).

Figure A2 - Illustration of the polymer blend film and an oxygen scavenging particle behavior in the reaction (Adapted from Carranza et al., 2010).

Figure A3 - Illustration of the polymer barrier formed by inert layers of thickness L_M and reactive layers of thickness L_R , where are the reactive particles (Adapted from Carranza et al., 2012).

Figure A4 - Configuration of three-layer film used in the oxygen transfer model. (Adapted from Di Maio, Marra, Bedane, et al., 2017).

LISTA DE TABELAS

Tabela 1 - Parâmetros e constantes utilizados no modelo proposto neste trabalho.

Table A1 - Thermoplastic materials for food packaging and its applications.

Table A2 - Oxygen scavenging systems for food package uses.

Table A3 - Mathematical models of oxygen transport in active polymeric films.

SUMÁRIO

1 INTRODUÇÃO	13
2 METODOLOGIA	15
2.1 DESCRIÇÃO DO MODELO	15
2.2 CONDIÇÕES INICIAL E DE CONTORNO	16
2.3 PARÂMETROS E CONSTANTE	17
2.4 SOLUÇÃO NUMÉRICA	17
3 RESULTADOS E DISCUSSÕES	19
4 CONSIDERAÇÕES FINAIS	25
APÊNDICE 1	26
REFERÊNCIAS	27

ANEXO - Review Article: Applications and oxygen transfer models in active multilayer food packaging: a theoretical review	29
A1 INTRODUCTION	31
A2 OXYGEN BARRIER PACKAGES	33
A2.1 POLYMER MATERIALS FOR FOOD PACKAGING	33
A2.2 OXYGEN BARRIERS SYSTEMS AND MECHANISMS	36
A.2.2.1 Oxygen Scavenger.....	37
A3 MATHEMATICAL MODELING AND SIMULATION OF OXYGEN-SCAVENGING POLYMERIC SYSTEMS	43
A3.1 DIFFUSION THEORY	43
A3.2 ACTIVE POLYMERIC SYSTEMS MODELING	44
A4 CONCLUSIONS	50
REFERENCES	52

INTRODUÇÃO

A embalagem tem como principal função a preservação da qualidade dos alimentos, promovendo proteção física (contra choques e luz), proteção contra agentes biológicos ou proteção química, como a transferência de pequenas moléculas de vapor de água, gases e compostos aromáticos (Restuccia et al., 2015; Wani et al., 2014), além da informação e conveniência no manuseio, garantindo uma relação custo-benefício e todos os aspectos da segurança alimentar (Anukiruthika et al., 2020). Os polímeros termoplásticos oferecem uma ampla gama de propriedades térmicas, mecânicas e de barreira, além de serem leves, transparentes e terem facilidade de processamento (Geueke et al., 2018; Kirwan et al., 2011; Silvestre et al., 2011). Eles podem ser classificados como polímeros barreira (EVOH, PDVC, PA6), quando apresentam permeabilidade baixa ao oxigênio, dióxido de carbono e aromas, ou como polímeros estruturais (PP, PE, PET), quando apresentam maior resistência mecânica e térmica, resistindo a processos como congelamento, esterilização e micro-ondas (Lechevalier, 2016). Todas essas propriedades são difíceis de se obter por apenas um material, por isso embalagens multicamadas vêm sendo desenvolvidas nas últimas décadas, a fim de que cada camada passiva forneça as propriedades de cada polímero utilizado na estruturação da embalagem (Noriega et al., 2014). Os sistemas multicamadas também podem conter substâncias ou aditivos que tenham alguma interação com o alimento ou a atmosfera que o permeia, capturando ou liberando moléculas de interesse, tornando esse sistema ativo (Dury-Brun et al., 2007). Essas soluções prolongam o prazo de validade e melhoram a qualidade e a segurança dos alimentos (Han et al., 2018). As embalagens multicamadas existentes no mercado mais aplicadas para embalagem de alimentos consistem de 3 a 7 camadas (Anukiruthika et al., 2020), .

A capacidade do polímero que compõe a embalagem de promover ou de limitar trocas de gás e vapor entre alimentos e o ambiente é um objeto de estudo importante, visto que, para alguns alimentos específicos, a limitação desse permeante reduz a degradação química e biológica, o crescimento microbiológico e a preservação das propriedades organolépticas (Noriega et al., 2014). Entretanto, um polímero com boa barreira ao oxigênio, por exemplo, pode apresentar baixa barreira à água e/ou perder suas propriedades de barreira com a umidade, como o copolímero de etileno e álcool vinílico (EVOH), enquanto o Polietileno (PE) que é apolar (hidrofóbico) e, portanto, boa barreira a umidade (Crippa et al., 2008; Marsh, 2016). As embalagens poliméricas multicamadas oferecem

funcionalidades adicionais, combinando propriedades funcionais, altas barreiras contra gases e vapor de água, mesmo com espessura reduzida, tornando possível a produção de embalagens mais finas, leves e compactas (Anukiruthika et al., 2020; Crippa et al., 2007). Diversas técnicas para o desenvolvimento de embalagens foram aplicadas nas últimas décadas, devido ao significativo papel desempenhado pelo oxigênio na deterioração dos alimentos, como oxidação lipídica, atividade enzimática, degradação de vitaminas, crescimento de microrganismos de deterioração e patogênicos (Van Bree et al., 2010).

O mecanismo de difusão de gases em materiais poliméricos foi descrito por Thomas Graham, que propôs que o processo de permeação envolvia a dissolução do gás com posterior passagem das espécies dissolvidas através da membrana (McKeen, 2012) e ocorre em três etapas: (1) adsorção e solubilização do permeante, ou seja, da molécula gasosa na superfície; (2) difusão do permeante através do material polimérico e (3) dessorção e evaporação do permeante na outra face do material (Belay et al., 2016; Mangaraj et al., 2009; Morris, 2017). Esse mecanismo é descrito pelas leis de Henry e Fick, em que se pode obter a expressão que relaciona a taxa de permeação com a área e a espessura no filme. Dessa maneira, entende-se que o conceito de permeabilidade está associado à avaliação das propriedades de barreira de um material plástico (Siracusa, 2012), as propriedades do penetrante e as condições ambientais em que se encontram (Lechevalier, 2016).

Para se determinar as melhores estruturas, que tenham a capacidade de barreira exigida para determinados alimentos e com menor custo possível, são necessários vários testes de materiais e espessuras diferentes. A modelagem matemática e simulação numérica têm sido grandes aliadas para prever o comportamento do oxigênio frente a esses diferentes materiais e configurações de camadas, incluindo também estudos com absorvedores de oxigênio incorporados a essas embalagens. As metodologias utilizadas para simular o comportamento do oxigênio nesses trabalhos contam com métodos analíticos para resolução das equações diferenciais do modelo, assim como *softwares* específicos para aplicação dos dados e simulação dos resultados (Carranza et al., 2010, 2012; Di Maio et al., 2017; Ferrari et al., 2009).

A Transformada de Laplace é uma técnica já estabelecida para soluções de equações diferenciais. Em várias circunstâncias as transformadas de uma função e suas inversas podem ser tabuladas. Porém, em muitas situações práticas, o uso de tabelas de transformações inversas e o uso de fórmulas de inversão não são adequados, sendo necessária uma inversão numérica (Davies & Crann, 1999).

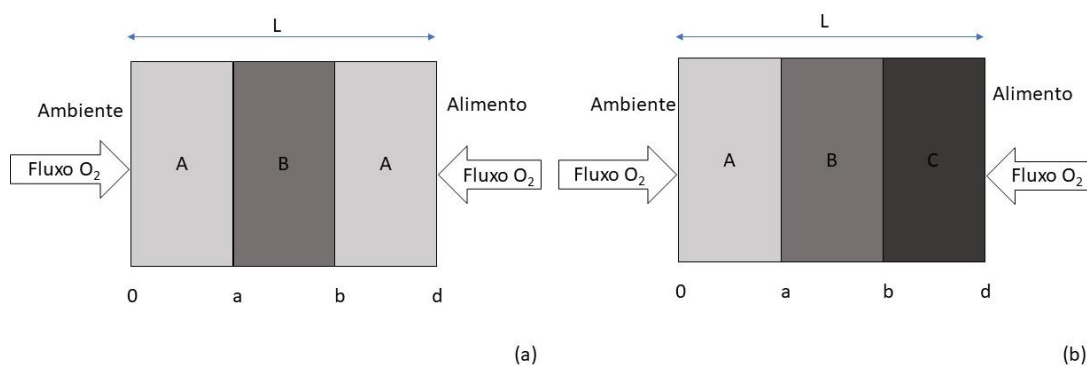
O objetivo deste trabalho foi predizer e comparar a concentração de oxigênio que permeia um filme multicamadas com diferentes materiais e espessuras, através de uma ferramenta de simulação numérica, a fim de selecionar materiais e configurações adequadas para embalagens de alimentos. A aplicação da ferramenta desenvolvida, utilizando a Transformada de Laplace aliada à um código para inversão numérica de Stehfest (Stehfest, 1970) e o método de Gauss-Siedel, possibilitou a observação da concentração de oxigênio através das camadas simuladas por meio de um compilador para *Fortran* 77 gratuito. Aplicando-se para diferentes materiais poliméricos com barreiras ao oxigênio distintas, é possível escolher o melhor material para cada tipo de alimento, visto que cada um tem uma necessidade diferente.

2 METODOLOGIA

2.1 DESCRIÇÃO DO MODELO

A estrutura selecionada como objeto de estudo foi um filme de espessura L , composto por três camadas, em configurações tipo ABA (figura 1a), com dois materiais diferentes, ou ABC (figura 1b), com os três materiais diferentes. O fluxo de oxigênio foi avaliado apenas em uma direção (x), sendo observada a concentração do meio externo (contato com o ambiente, $x=0$) e do meio interno (contato com o alimento, $x=d$) da embalagem. A estrutura escolhida foi resultado de uma análise de trabalhos descritos na literatura (Apicella et al., 2018; Di Maio et al., 2017), bem como das embalagens utilizadas comercialmente pelas indústrias de alimentos (Anukiruthika et al., 2020).

Figura 1. Representação do filme multicamadas com configurações ABA (a) e ABC (b).



Fonte: Elaborado pelo autor.

A segunda Lei de Fick descreve a difusão em um estado não-estacionário, em que o gradiente de concentração da substância difundida é uma função do tempo. Na ausência de quaisquer reações químicas e considerando o fluxo apenas em uma direção (x), temos:

$$\frac{\partial C}{\partial t} = D \frac{\partial^2 C}{\partial x^2} \quad (1)$$

em que C (mol/cm^3) é a concentração da substância difundida (oxigênio), t (s) é o tempo em que o processo de difusão do oxigênio ocorre, x (cm) é o espaço coordenado unidimensional medido na seção do material polimérico e D (cm^2/s) é o coeficiente de difusão da molécula gasosa no polímero.

As equações da difusão para cada camada do filme polimérico do presente estudo são dadas por:

$$\frac{\partial C_1}{\partial t} = D_1 \frac{\partial^2 C_1}{\partial x^2} \quad 0 < x \leq a, t > 0 \quad (2)$$

$$\frac{\partial C_2}{\partial t} = D_2 \frac{\partial^2 C_2}{\partial x^2} \quad a < x \leq b, t > 0 \quad (3)$$

$$\frac{\partial C_3}{\partial t} = D_3 \frac{\partial^2 C_3}{\partial x^2} \quad b < x \leq d, t > 0 \quad (4)$$

2.2 CONDIÇÕES INICIAL E DE CONTORNO

Como condição inicial foi considerada ausência de oxigênio em todas as camadas ($C_{oxy}(x,0) = 0$). Dada a estrutura do filme multicamadas e a configuração do arranjo, a simetria do perfil de concentração do oxigênio foi estabelecida na sessão intermediária da camada 2, enquanto nas superfícies externas do filme foi considerada a seguinte condição:

$$C_1(0,t) = C_3(d,t) = sC_{oxy} \quad t > 0 \quad (5)$$

em que, C_{oxy} é a concentração de oxigênio que irá permear no material (A ou C) e s é o coeficiente de solubilidade do oxigênio. Respeitando a continuidade do fluxo de massa nas interfaces entre as camadas, temos as seguintes condições:

$$C_1(a,t) = C_2(a,t) \quad t > 0 \quad (6)$$

$$C_2(b,t) = C_3(b,t) \quad t > 0 \quad (7)$$

$$D_1 \frac{\partial C_1}{\partial x} = D_2 \frac{\partial C_2}{\partial x} \quad t > 0 \quad (8)$$

$$D_2 \frac{\partial C_2}{\partial x} = D_3 \frac{\partial C_3}{\partial x} \quad t > 0 \quad (9)$$

2.3 PARÂMETROS E CONSTANTES

Os parâmetros e constantes utilizados no presente estudo (tabela 1) são descritos na literatura (Di Maio et al., 2017; Keller & Kouzes, 2017), compreendendo os coeficientes de difusão para cada material, a solubilidade do oxigênio e a concentração inicial de oxigênio (concentração de O₂ ambiente). O PET e PE representam a grande maioria dos polímeros utilizados como embalagem de alimentos, e o EVOH é um dos que apresenta maior barreira ao oxigênio (Robertson, 2013; Morris, 2017).

A espessura das três camadas do filme polimérico foi fixada em 13µm, 9µm, 13µm para as camadas 1, 2 e 3, respectivamente, totalizando 35µm, configuração também utilizada no estudo de Di Maio, et al., (2017), em que simulava o uso para frutas e vegetais minimamente processados.

Tabela 1 – Parâmetros e constantes utilizados no modelo proposto neste trabalho.

Descrição	Parâmetro	Valor	Unidade
Coeficiente de difusão do O₂ em PET (23 °C; 1 atm)	D _{PET}	2,71x10 ⁻⁹	cm ² /s
Coeficiente de difusão do O₂ em EVOH (25 °C; 1 atm)	D _{EVOH}	7,2x10 ⁻¹⁰	cm ² /s
Coeficiente de difusão do O₂ em PE (25 °C; 1 atm)	D _{PE}	1,0x10 ⁻⁶	cm ² /s
Coeficiente de difusão do O₂ em PP (25°C; 1 atm)	D _{PP}	3,76x10 ⁻⁷	cm ² /s
Coeficiente de solubilidade do O₂ (23 °C; 1 atm)	s	7,16x10 ⁻²	cm ³ /cm ³ /bar
Concentração inicial do O₂ em t=0	C _{oxy}	8,561x10 ⁻³	mol/L

PET: Polietileno tereftalato; EVOH: Copolímero de etileno e álcool vinílico; PE: Polietileno; PP: Polipropileno. Fonte: Elaborada pelo autor.

2.4 SOLUÇÃO NUMÉRICA

Nas equações de cada camada do filme polimérico (2, 3 e 4), bem como nas condições inicial e de contorno (5 a 9), foi aplicada a transformada de Laplace analítica, convertendo-se nas equações 10 a 17, em que *p* é o parâmetro de Laplace

$$\frac{d^2\bar{C}_1}{dx^2} - q_1^2\bar{C}_1 = 0 \quad 0 \leq x \leq a, q_1 = \sqrt{\frac{p}{D_1}} \quad (10)$$

$$\frac{d^2\bar{C}_2}{dx^2} - q_2^2\bar{C}_2 = 0 \quad a < x \leq b, q_2 = \sqrt{\frac{p}{D_2}} \quad (11)$$

$$\frac{d^2\bar{C}_3}{dx^2} - q_3^2\bar{C}_3 = 0 \quad b < x \leq d, q_3 = \sqrt{\frac{p}{D_3}} \quad (12)$$

$$\mathcal{C}_1(0) = \mathcal{C}_3(d) = s\mathcal{C}_{oxy} = \frac{R}{p}, \quad R = s\mathcal{C}_{oxy} \quad (13)$$

$$\bar{\mathcal{C}}_1(a) = \bar{\mathcal{C}}_2(a) \quad (14)$$

$$\bar{\mathcal{C}}_2(b) = \bar{\mathcal{C}}_3(b) \quad (15)$$

$$D_1 \frac{d\bar{\mathcal{C}}_1}{dx} \Big|_{x=a} = D_2 \frac{d\bar{\mathcal{C}}_2}{dx} \Big|_{x=a} \quad (16)$$

$$D_2 \frac{d\bar{\mathcal{C}}_2}{dx} \Big|_{x=b} = D_3 \frac{d\bar{\mathcal{C}}_3}{dx} \Big|_{x=b} \quad (17)$$

As equações 10, 11 e 12 foram resolvidas analiticamente, resultando em

$$\bar{\mathcal{C}}_1(x) = Ae^{q_1x} + Be^{-q_1x} \quad (18)$$

$$\bar{\mathcal{C}}_2(x) = Ce^{q_2x} + De^{-q_2x} \quad (19)$$

$$\bar{\mathcal{C}}_3(x) = Ee^{q_3x} + Fe^{-q_3x} \quad (20)$$

Aplicando as condições 13 a 17 nas EDOs (10 a 12) e fazendo as devidas substituições, temos

$$\bar{\mathcal{C}}_1(x) = \frac{R}{p}e^{q_1x} - H \sinh(q_1x) \quad (21)$$

$$\bar{\mathcal{C}}_2(x) = Ce^{q_2x} + De^{-q_2x} \quad (22)$$

$$\bar{\mathcal{C}}_3(x) = G \sinh(q_3(x-d)) \quad (23)$$

sendo descritas no Apêndice 1 os coeficientes H, C, D e G.

Devido à complexidade das equações, quando substituímos os coeficientes, a obtenção analítica das transformadas inversas de Laplace seria muito onerosa de se desenvolver, por isso foi necessária a implementação da transformada inversa de forma numérica. Um algoritmo para o cálculo numérico da inversa de Laplace foi adaptado (Stehfest, 1970), onde a aproximação se dá pela escolha de um conjunto de M valores para o parâmetro de Laplace, em que T é o tempo de simulação

$$p_j = j \frac{\ln 2}{T} \quad j = 1, 2, \dots, M \quad (24)$$

sendo M um valor par. A expressão para a inversão numérica a partir da Transformada de Laplace é dada por

$$f(T) \approx \frac{\ln 2}{T} \sum_{j=1}^M w_j F(p_j) \quad \text{para } T = t \quad (25)$$

sendo a matriz w_j dada por

$$w_j = (-1)^{(M/2)+j} \sum_{k=\lceil \frac{1+j}{2} \rceil}^{\min(j, M/2)} \frac{(2k)! k^{M/2}}{\left(\frac{M}{2}-k\right)! k! (k-1)! (j-k)! (2k-j)!} \quad (26)$$

em que k deve ser o menor número inteiro da operação.

O método de Stehfest é aplicável para funções mais simples. No caso de um problema de valor de contorno aplicado à difusão, como neste trabalho, é adequada a associação do método de diferenças finitas com o algoritmo de Stehfest e o método de Gauss-Siedel, a fim de evitar instabilidades numéricas (Davies & Crann, 1999).

Com a definição das equações para inversão de Laplace através dos métodos descritos anteriormente, um código numérico foi escrito em linguagem *Fortran 77*, em um compilador livre (*gFortran®*) em *Linux®*, em que foi possível obter os resultados gráficos (figuras 2 a 6), para o perfil de concentração de oxigênio ao longo da espessura do filme polimérico composto por três camadas, que serão discutidos na próxima sessão.

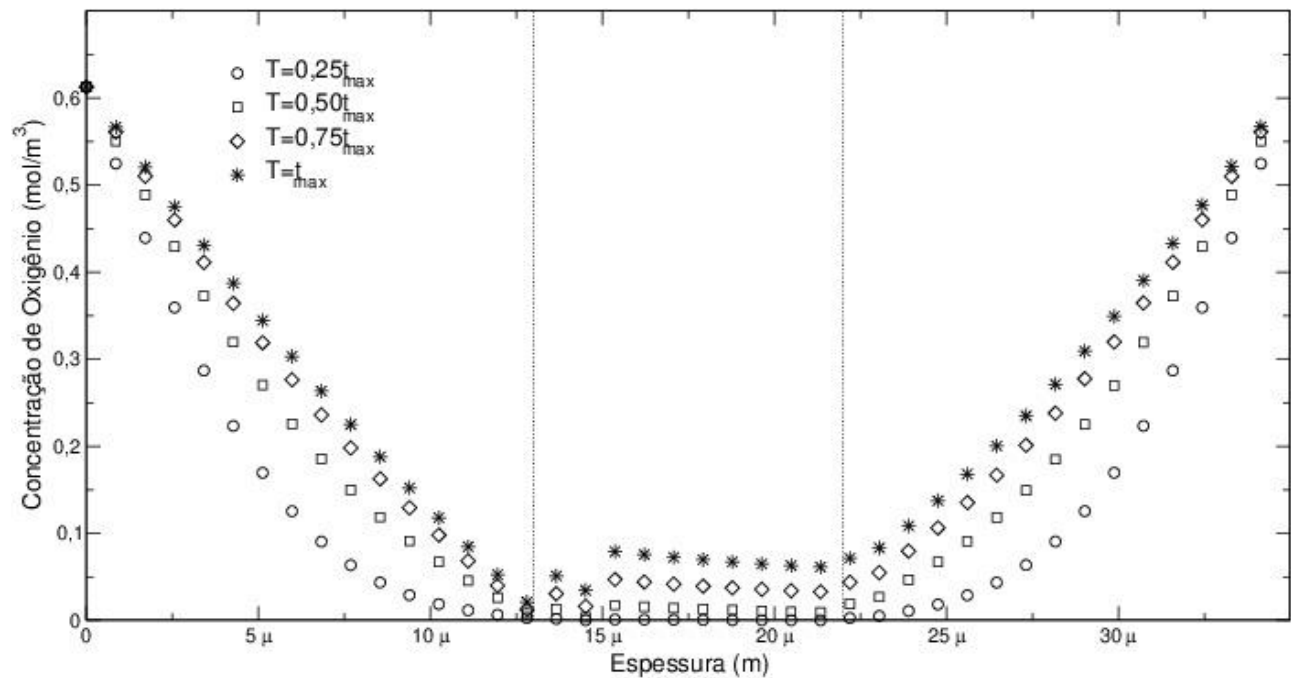
3 RESULTADOS E DISCUSSÕES

Dois parâmetros importantes foram testados a fim de melhorar a estabilidade do código numérico implementado. O valor de M é muito significativo no processo de inversão numérica e a escolha adequada deste define a precisão do método, pois um dado incorreto poderá ocasionar problemas de arredondamento nesse processo. Davies & Crann (1999) destacam ser mais apropriados $M = 6, 8$ ou 16 , porém não é possível afirmar um valor ótimo para este parâmetro, pois a escolha dele depende do problema estudado. Assim, no presente trabalho foram testados $4, 6, 8, 10, 16$ e 24 e o parâmetro $M = 8$ foi o que apresentou melhor estabilidade numérica. Para valores de M maiores, verificou-se que w_j tornava-se muito grande numericamente, o que provocava a instabilidade no processo, devido à falta de limites do operador inverso de Laplace. Outro parâmetro testado foi o tempo máximo de simulação numérica (t_{max}). Quando valores de tempo de simulação numérica (T) muito grandes ($T \rightarrow t_{max}$) foram utilizados (equação 12), o valor de p_j tornou-se muito pequeno, provocando divergências. A partir da definição de $t_{max} = 0,5$, foram traçadas curvas com $T = 0,25t_{max}$, $T = 0,50t_{max}$, $T = 0,75t_{max}$ e $T = t_{max}$. A partir de um determinado valor o sistema entra em equilíbrio e a curva não se modifica, ou seja, as curvas de evolução não se distinguem. Os parâmetros definidos para M e t_{max} são os mesmos para todas as simulações.

O modelo semi-analítico foi testado para prever a capacidade de barreira de filmes multicamadas para aplicação em embalagem de alimentos. Com as soluções numéricas foi possível

obter o perfil de concentração de oxigênio ao longo da espessura do filme para cada configuração selecionada (ABA ou ABC), representados nas figuras 2 a 6, sendo as linhas verticais a interface entre as camadas. Na figura 2 pode-se observar que os perfis de concentração de oxigênio nas camadas externas apresentaram o mesmo comportamento, já que se tratava do mesmo material (configuração ABA), o Polietileno, que apresenta mesmo coeficiente de difusão (D_{PE} : $1,0 \cdot 10^{-6} \text{ cm}^2/\text{s}$), enquanto o coeficiente de difusão da camada interna, composta por Copolímero de Etileno e Álcool Vinílico, é na ordem de 10^4 vezes menor (D_{EVOH} : $7,2 \cdot 10^{-10} \text{ cm}^2/\text{s}$). É possível observar uma pequena oscilação no perfil de concentração na interface entre as camadas A e B desta configuração (figura 2) para as curvas com $T=0,50t_{\max}$, $0,75t_{\max}$ e t_{\max} , provavelmente por limitações da metodologia utilizada, que ocasionaram uma flutuação numérica na função concentração quando migrava de material, devido ao EVOH apresentar uma barreira maior ao oxigênio que o PE. Já quando o tempo de simulação foi de $0,25t_{\max}$, a curva não apresentou a oscilação.

Figura 2 – Perfil de concentração do oxigênio no interior de filme multcamada composto por PE/EVOH/PE – configuração ABA.

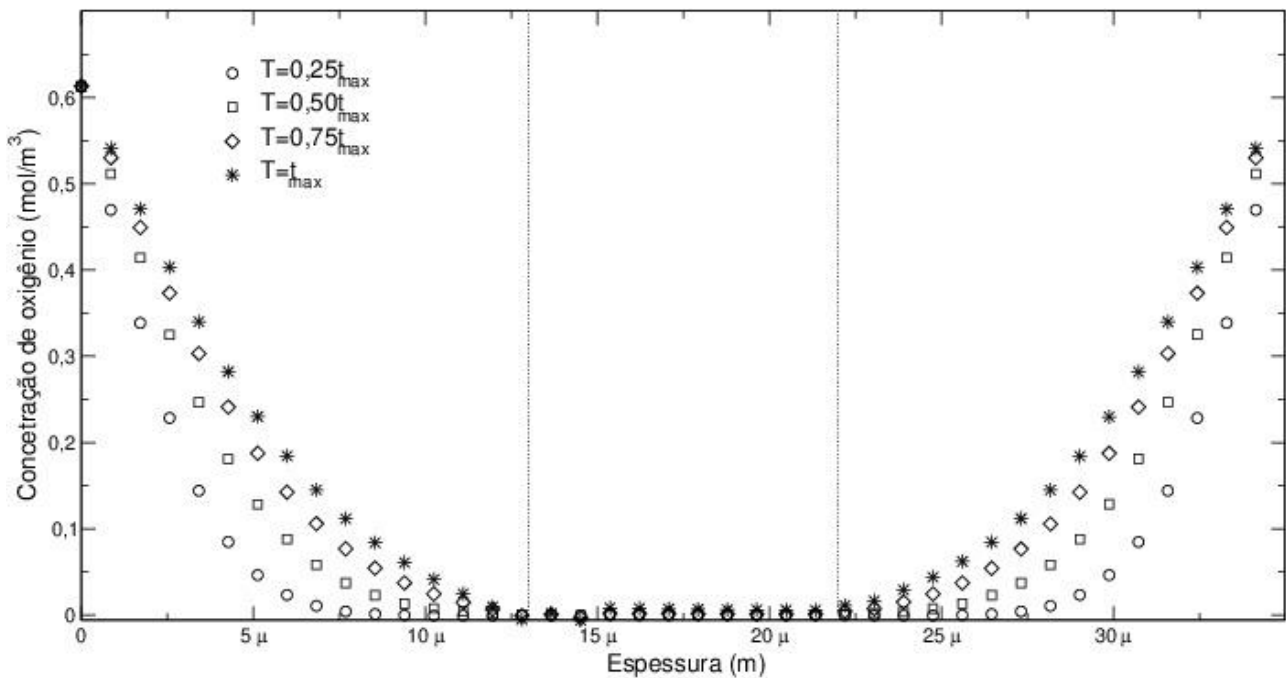


Fonte: Elaborado pelo autor com *Xmgrace*®.

O mesmo comportamento simétrico para o perfil de concentração é observado na figura 3, que apresenta a configuração ABA, porém com as camadas externas substituídas por Polipropileno (D_{PP} : $3,76 \cdot 10^{-7} \text{ cm}^2/\text{s}$), enquanto a interna permaneceu com EVOH. Houve uma pequena mudança

no perfil de concentração, possivelmente pela diferença na variação entre os coeficientes de difusão que, neste caso, da camada externa é na ordem de 10^3 vezes maior que a interna. Nesta configuração as oscilações nas interfaces das camadas percebidas foram mais brandas e na camada B as curvas traçadas para os diferentes tempos de simulação se sobrepuiseram. A metodologia desenvolvida foi capaz de simular o comportamento do oxigênio frente ao sistema multicamadas, sem que houvesse variação na função concentração.

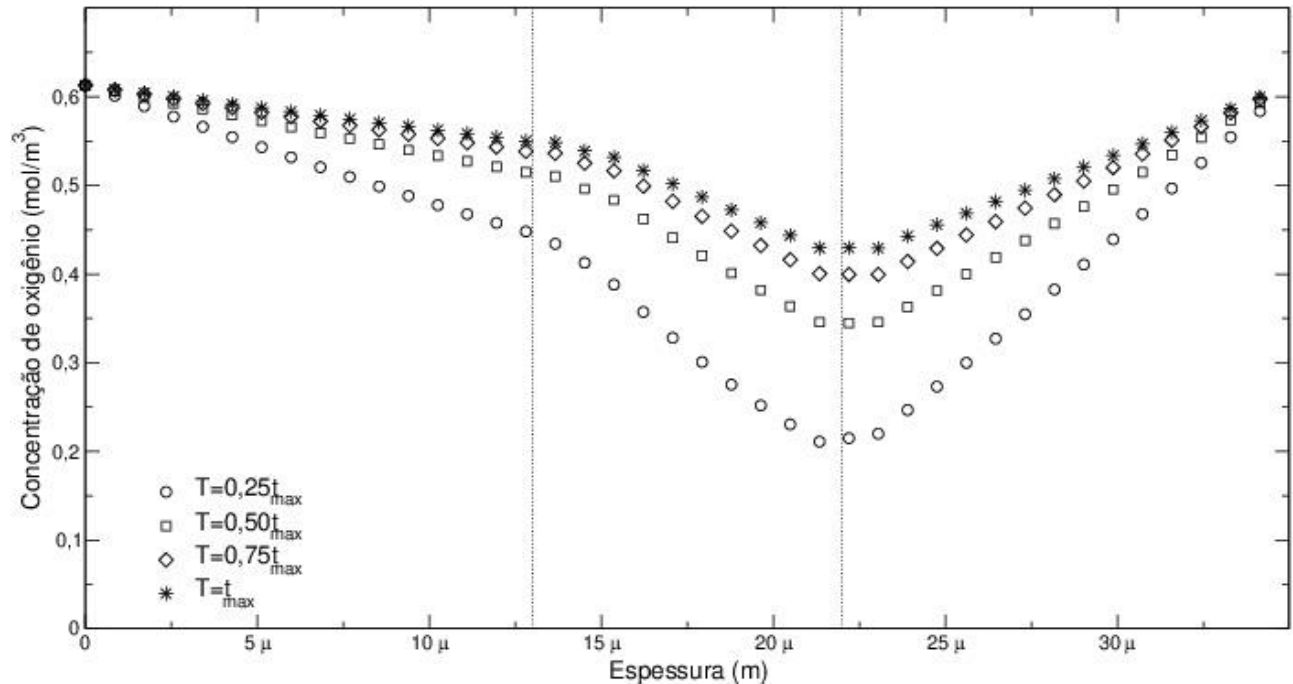
Figura 3 – Perfil de concentração do oxigênio no interior de filme multicamada composto por PP/EVOH/PP - configuração ABA.



Fonte: Elaborado pelo autor com *Xmgrace*[®].

A diferença entre ordem de grandeza na difusividade dos materiais afeta a concentração de oxigênio nas camadas vizinhas. Nas figuras 2 e 3, em que as camadas externas apresentam coeficiente de difusão 10^4 e 10^3 vezes maior que a camada interna, respectivamente, a concentração de oxigênio decai rapidamente, sem ocorrer flutuação numérica na função concentração, assim como na camada C da configuração mostrada na figura 6. Já quando a diferença entre a difusividade de cada material é pequena, na ordem de 10 vezes, como na figura 4, o perfil de concentração tem uma inclinação menor, principalmente para tempos de simulação maiores, um comportamento esperado, devido ao fato de a capacidade de barreira dos materiais apresentarem-se mais aproximados.

Figura 4 – Perfil de concentração do oxigênio no interior de filme multicamada composto por PET/EVOH/PET - configuração ABA.

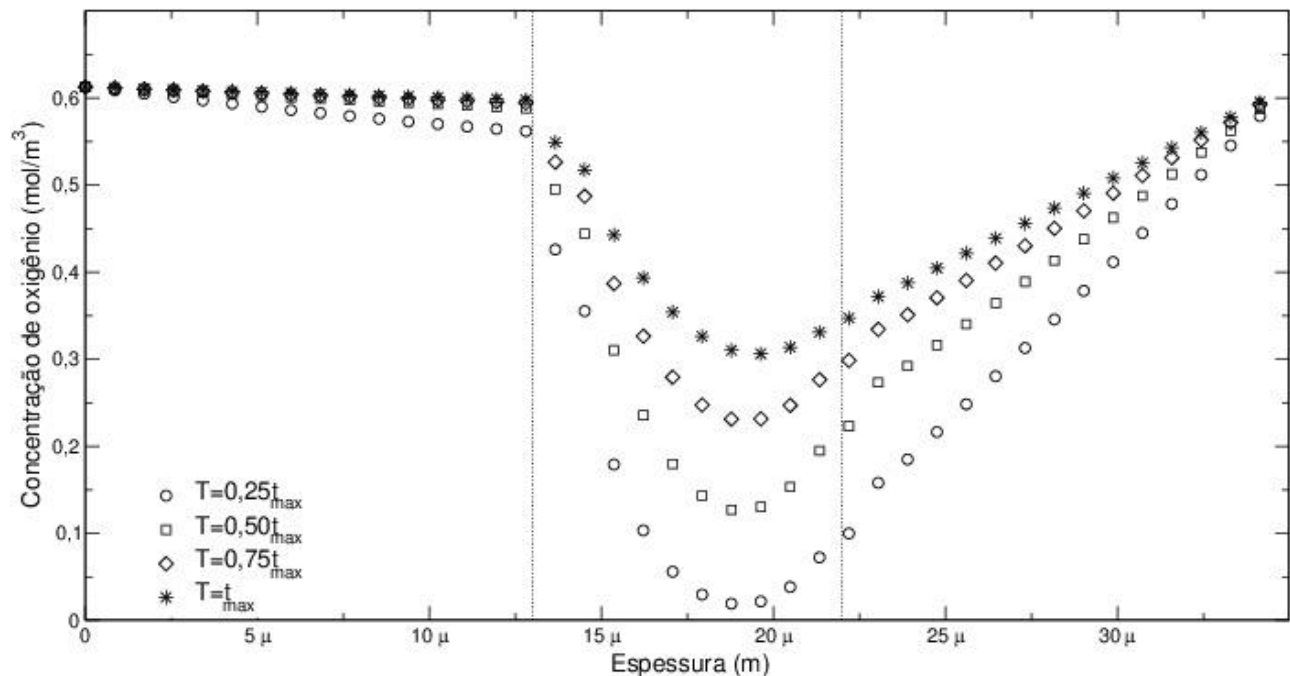


Fonte: Elaborado pelo autor com *Xmgrace*®.

Outro fato observado na simulação numérica da figura 4 é o deslocamento da curva simétrica que observamos nas figuras 2 e 3. Neste caso em que as difusividades dos materiais são de ordem de grandeza mais próxima, é possível verificar mais claramente a interferência da vizinhança no perfil de concentração do oxigênio ao longo de cada camada do filme, visto que a simulação numérica sempre inicia em $x = 0$ (contato com o ambiente) e os pontos são calculados para o sentido da parte interna da embalagem (contato com o alimento). Esse comportamento também foi percebido de maneira mais proeminente quando o material da camada intermediária foi substituído por um filme com difusividade maior que das camadas externas como o Polipropileno (PP), na figura 5. Conforme o tempo de simulação foi diminuído ($T = 0,25t_{\max}$ e $0,50t_{\max}$), maior foi a decaimento da curva quando o perfil de concentração migrava do material A para o material B. Todas as configurações testadas na configuração ABA apresentaram oscilações quando a difusão acontece do material A (contanto

com a ambiente) para o material B (intermediária), na primeira interface, na qual o oxigênio encontra uma barreira maior na segunda camada, pois o coeficiente de difusão do material A é maior que do material B. Já quando o oxigênio se difundia da camada B (intermediária) para a camada A (contato com o alimento), na segunda interface da embalagem, não houve oscilações, pois, a barreira da terceira camada da embalagem era menor, facilitando o transporte do oxigênio.

Figura 5 – Perfil de concentração do oxigênio no interior de filme multicamada composto por PET/PP/PET - configuração ABA.

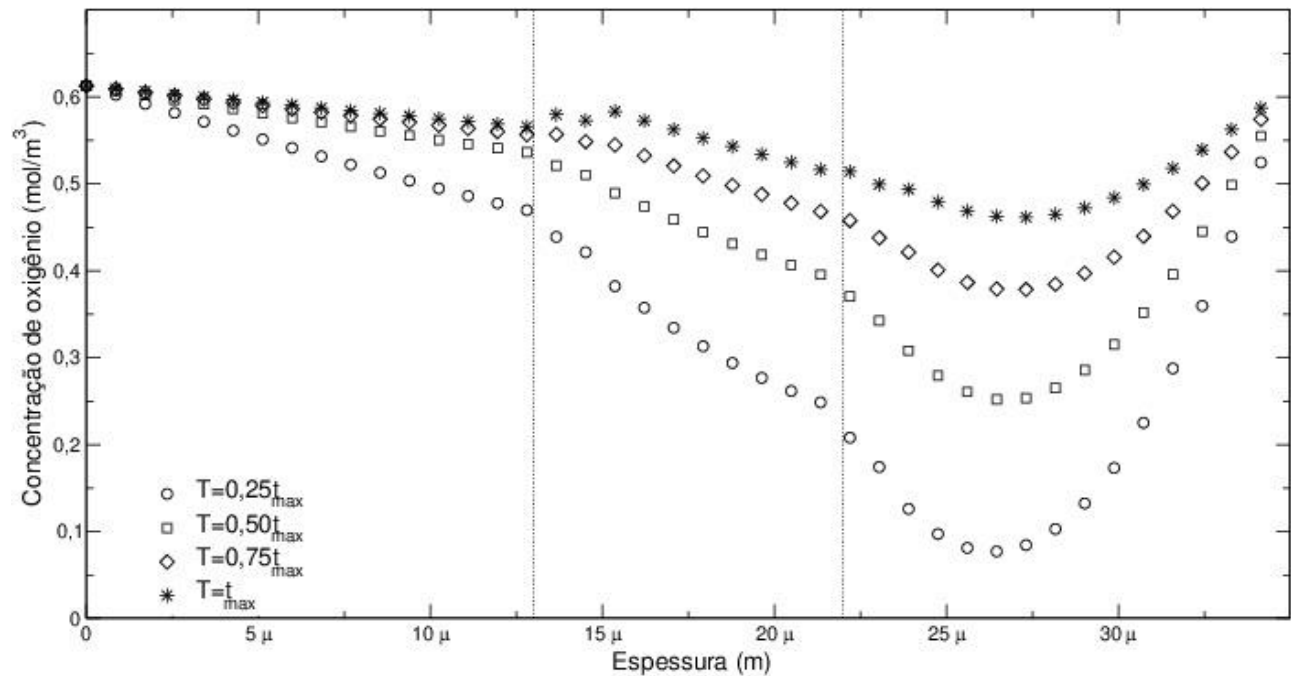


Fonte: Elaborado pelo autor com *Xmgrace*[®].

Em filmes em que a configuração das camadas testada foi ABC, um comportamento gráfico assimétrico foi observado, pois, nesses casos, há três materiais que apresentam difusividades distintas. A figura 6 representa esse comportamento, em que os polímeros PET, EVOH e PE têm coeficientes de difusão $2,7 \times 10^{-9} \text{ cm}^2/\text{s}$, $7,2 \times 10^{-10} \text{ cm}^2/\text{s}$ e $1,0 \times 10^{-6} \text{ cm}^2/\text{s}$, respectivamente. Esse mesmo comportamento foi observado em um estudo utilizando o *software* comercial baseado no método de elementos finitos, o *Comsol*[®], que apresentava como camadas externas PET e PE, como na configuração da figura 6, porém a camada intermediária do estudo incluía um absorvedor de oxigênio, que reduziu a concentração de oxigênio a zero nesta camada (Di Maio et al., 2017), enquanto o presente estudo apresenta um material inerte, mas com coeficiente de difusão menor que o material das camadas externas. O comportamento gráfico do estudo citado pode ser associado às curvas

obtidas no presente estudo, quando comparados nos tempos de simulação menores ($0,25t_{\max}$ e $0,50t_{\max}$).

Figura 6 – Perfil de concentração do oxigênio no interior de filme multicamada composto por PET/EVOH/PE - configuração ABC.



Fonte: Elaborado pelo autor com *Xmgrace*®.

Nesta última simulação pode-se observar que também houve uma pequena flutuação nos primeiros pontos da camada B (EVOH), onde a concentração de oxigênio aumenta no início da camada e depois volta a diminuir. Esse comportamento foi observado para tempos de simulação maiores ($0,75t_{\max}$ e t_{\max}), reforçando novamente que para tempos de simulação menores, a instabilidade numérica diminui e é possível obter perfis de concentração de oxigênio, sem que ocorra a oscilação na função quando a difusão é analisada em materiais multicamadas.

A concentração de oxigênio num ponto é calculada pela concentração dada num ponto antes e um ponto depois, pelo método de Gauss-Siedel. Logo, nas interfaces das camadas, a concentração é calculada a partir da equação que corresponde à camada de um material (A ou B) e a concentração que corresponde à camada de outro material (B ou C). A cada iteração, a aproximação encontrada é testada, para verificar se esta pode ser considerada a solução do problema, através de uma análise de erro numérico, que deve ser menor ou igual a 10^{-5} mol/m^3 . Verificando ainda as equações 21 a 23, obtidas nas soluções no espaço de Laplace e utilizadas para o cálculo da concentração de oxigênio,

também há interação entre os dados de cada material no material vizinho. Diante disso, vemos a influência que uma camada tem sobre a outra e isso pode estar ocasionando essas oscilações, como observado nas figuras 2 e 6, pois temos influência tanto das soluções analíticas obtidas, que carregam dados do material próximo, como pelo método de Gauss-Siedel. Reiterando que essas oscilações ocorrem para tempo de simulação maiores, logo, o uso de tempos menores de simulação numérica se torna mais adequado para convergência dos resultados, gerando perfis de concentração de oxigênio sem as flutuações numéricas na função concentração.

4 CONSIDERAÇÕES FINAIS

A metodologia proposta foi capaz de simular o perfil de concentração do oxigênio frente a alguns materiais poliméricos selecionados, através de uma linguagem de programação de alto nível, utilizando um compilador livre. Esta ainda pode ser aperfeiçoada, visto que para algumas configurações foram detectadas oscilações numéricas, quando o tempo de simulação era aumentado. Logo, uma análise mais minuciosa deve ser realizada a fim de diminuir essa instabilidade do método. A Transformada de Laplace é amplamente utilizada para resolução de equações diferenciais e foi utilizada no presente trabalho para resolver a equação da difusão num estado não estacionário (2^a Lei de Fick). A utilização de uma ferramenta de simulação numérica que possa calcular a sua inversa amplia sua aplicação a problemas encontrados na engenharia.

A ferramenta desenvolvida e utilizada no presente estudo se mostrou promissora para aplicação no estudo da difusão em sistemas poliméricos multicamadas e pode ser estendida para descrever outros sistemas, com mais camadas que os manipulados nesta pesquisa. O comportamento gráfico para simulação numérica pode ser facilmente comparado com resultados experimentais e simulados descritos na literatura. Os *softwares* utilizados nas pesquisas descritas na literatura (*Comsol®*, *MATLAB®* e *Maplesoft®*) são geralmente pagos, fazendo necessário o uso de mais recursos por parte do pesquisador. A metodologia elaborada foi de baixo custo, visto que os *softwares* utilizados (*gFrotran®* e *Xmgrace®*) são gratuitos, demandando de tempo, conhecimento matemático e de programação para elaboração. Trabalhos futuros podem contemplar tanto o aperfeiçoamento da metodologia desenvolvida quanto a ampliação do número de camadas do sistema de embalagem.

APÊNDICE 1- Coeficientes das funções concentração obtidas no espaço de Laplace, para as três camadas do sistema de embalagem simulado.

$$G = \frac{\omega}{1 - \delta - \xi} \quad (1)$$

$$C = \varphi + G\tau \quad (2)$$

$$D = \rho - G\sigma \quad (3)$$

$$H = \alpha C - \beta D - \gamma \quad (4)$$

$$\alpha = \frac{-D_2 q_2 e^{q_2 a}}{D_1 q_1 \cosh(q_1 a)} \quad (5)$$

$$\beta = \frac{-D_2 q_2 e^{-q_2 a}}{D_1 q_1 \cosh(q_1 a)} \quad (6)$$

$$\gamma = \frac{-R e^{q_2 a}}{p \cosh(q_1 a)} \quad (7)$$

$$\varepsilon = \frac{R}{p} e^{a(q_1+q_2)} - \gamma e^{q_2 a} \sinh(q_1 a) \quad (8)$$

$$\eta = \alpha e^{q_2 a} \sinh(q_1 a) + e^{2q_2 a} \quad (9)$$

$$\theta = \beta e^{q_2 a} \sinh(q_1 a) \quad (10)$$

$$\lambda = \frac{1 - \theta}{\eta} - e^{-2q_2 b} \quad (11)$$

$$\mu = e^{q_2 b} \sinh(q_3(b - d)) \quad (12)$$

$$\rho = \frac{\varepsilon}{\lambda \eta} \quad (13)$$

$$\sigma = \frac{\mu}{\lambda} \quad (14)$$

$$\varphi = \frac{\varepsilon - \rho - \rho \theta}{\eta} \quad (15)$$

$$\tau = \frac{\sigma - \sigma \theta}{\eta} \quad (16)$$

$$\rho = \frac{\varepsilon}{\lambda \eta} \quad (17)$$

$$\omega = \frac{D_2 q_2 e^{q_2 b} \varphi - D_2 q_2 e^{-q_2 b} \rho}{D_3 q_3 \cosh(q_3(b - d))} \quad (18)$$

$$\delta = \frac{D_2 q_2 e^{q_2 b} \tau}{D_3 q_3 \cosh(q_3(b - d))} \quad (19)$$

$$\xi = \frac{D_2 q_2 e^{-q_2 b} \sigma}{D_3 q_3 \cosh(q_3(b-d))} \quad (20)$$

5 REFERÊNCIAS

- Anukiruthika, T., Sethupathy, P., Wilson, A., Kashampur, K., Moses, J. A., & Anandharamakrishnan, C. (2020). Multilayer packaging: Advances in preparation techniques and emerging food applications. *Comprehensive Reviews in Food Science and Food Safety*, 19, 1156–1186. <https://doi.org/10.1111/1541-4337.12556>
- Apicella, A., Scarfato, P., Di Maio, L., & Incarnato, L. (2018). Transport properties of multilayer active PET films with different layers configuration. *Reactive and Functional Polymers*, 127, 29–37. <https://doi.org/10.1016/j.reactfunctpolym.2018.03.015>
- Belay, Z. A., Caleb, O. J., & Opara, U. L. (2016). Modelling approaches for designing and evaluating the performance of modified atmosphere packaging (MAP) systems for fresh produce: A review. *Food Packaging and Shelf Life*, 10, 1–15. <https://doi.org/10.1016/j.fpsl.2016.08.001>
- Carranza, S., Paul, D. R., & Bonnecaze, R. T. (2010). Analytic formulae for the design of reactive polymer blend barrier materials. *Journal of Membrane Science*, 360, 1–8. <https://doi.org/10.1016/j.memsci.2010.04.029>
- Carranza, S., Paul, D. R., & Bonnecaze, R. T. (2012). Multilayer reactive barrier materials. *Journal of Membrane Science*, 399–400, 73–85. <https://doi.org/10.1016/j.memsci.2012.01.030>
- Crippa, A., Sydenstricker, T. H. D., Amico, S., & C. (2007). Desempenho de filmes multicamadas em embalagens termoformadas. *Polímeros: Ciência e Tecnologia*, 17, 188–193. <https://doi.org/10.1590/s0104-14282007000300006>
- Crippa, A., Sydenstricker, T. H. D., & Amico, S. C. (2008). Evaluation of multilayer thermoformed films for food packaging. *Polymer - Plastics Technology and Engineering*, 47, 991–995. <https://doi.org/10.1080/03602550802353110>
- Davies, A., & Crann, D. (1999). The solution of differential equations using numerical Laplace transforms. *International Journal of Mathematical Education in Science and Technology*, 30(1), 65–79. <https://doi.org/10.1080/002073999288111>
- Di Maio, L., Marra, F., Bedane, T. F., Incarnato, L., & Saguy, S. (2017). Oxygen transfer in co-extruded multilayer active films for food packaging. *AICHE Journal*, 63(11), 5215–5221. <https://doi.org/10.1002/aic.15844>
- Dury-Brun, C., Chalier, P., Desobry, S., & Voilley, A. (2007). Multiple mass transfers of small volatile molecules through flexible food packaging. *Food Reviews International*, 23(3), 199–255. <https://doi.org/10.1080/87559120701418319>
- Ferrari, M. C., Carranza, S., Bonnecaze, R. T., Tung, K. K., Freeman, B. D., & Paul, D. R. (2009). Modeling of oxygen scavenging for improved barrier behavior: Blend films. *Journal of Membrane Science*, 329(1–2), 183–192. <https://doi.org/10.1016/j.memsci.2008.12.030>
- Geueke, B., Groh, K., & Muncke, J. (2018). Food packaging in the circular economy: Overview of chemical safety aspects for commonly used materials. *Journal of Cleaner Production*, 193, 491–505. <https://doi.org/10.1016/j.jclepro.2018.05.005>
- Han, J. W., Ruiz-Garcia, L., Qian, J. P., & Yang, X. T. (2018). Food Packaging: A Comprehensive Review and Future Trends. *Comprehensive Reviews in Food Science and Food Safety*, 17(4), 860–877. <https://doi.org/10.1111/1541-4337.12343>

- Keller, P. E., & Kouzes, R. T. (2017). *Water Vapor Permeation in Plastics*.
<https://doi.org/10.2172/1411940>
- Kirwan, M. J., Plant, S., & Strawbridge, J. W. (2011). Plastics in Food Packaging. In R. Coles & M. Kirwan (Eds.), *Food and Beverage Packaging Technology* (2th ed., pp. 157–212). Clackwell Publishing Ltd. <https://doi.org/10.1002/9781444392180>
- Lechevalier, V. (2016). Packaging: Principles and Technology. In R. Jeantet, T. Croguennec, P. Schuck, & G. Brulé (Eds.), *Handbook of Food Science and Technology: Food Process Engineering and Packaging* (1 ed., vol. 2, pp. 269–315). John Wiley & Sons, Inc.
<https://doi.org/10.1002/9781119285229.ch8>
- Marsh, K.S. (2016). Plastic Food Containers. *Reference Module in Food Science*, 1-4.
<http://dx.doi.org/10.1016/B978-0-08-100596-5.03196-6>
- Mangaraj, S., Goswami, T. K., & Mahajan, P. V. (2009). Applications of Plastic Films for Modified Atmosphere Packaging of Fruits and Vegetables: A Review. *Food Engineering Reviews*, 1, 133–158. <https://doi.org/10.1007/s12393-009-9007-3>
- McKeen, L. W. (2012). Introduction to Permeation of Plastics and Elastomers. In *Permeability Properties of Plastics and Elastomers* (3 ed., pp. 1–20). Elsevier Inc.
<https://doi.org/10.1016/b978-1-4377-3469-0.10001-3>
- Morris, B. A. (2017). Barrier. In *The Science and Technology of Flexible Packaging* (1 ed, pp. 259–308). Plastic Design Library. <https://doi.org/10.1016/B978-0-323-24273-8.00008-3>
- Noriega, M. D. P., Estrada, O., & López, I. (2014). Computational model to design plastic multi-layer films for food packaging to assure a shelf life at the best cost. *Journal of Plastic Film and Sheeting*, 30(1), 48–76. <https://doi.org/10.1177/8756087913484920>
- Restuccia, D., Puoci, F., Parisi, O. I., & Picci, N. (2015). Food Applications of Active and Intelligent Packaging: Legal Issues and Safety Concerns. In G. Cirillo, U. G. Spizzirri, & F. Iemma (Eds.), *Functional Polymers in Food Science* (1 ed., vol. 1, pp. 401–429). S.
<https://doi.org/10.1002/9781119109785.ch12>
- Robertson, G. L. (2013). Food Packaging: Principles and Practice, Third Edition. CRC Press LCC.
- Silvestre, C., Duraccio, D., & Cimmino, S. (2011). Food packaging based on polymer nanomaterials. *Progress in Polymer Science*, 36, 1766–1782.
<https://doi.org/10.1016/j.progpolymsci.2011.02.003>
- Siracusa, V. (2012). Food packaging permeability behaviour: A report. *International Journal of Polymer Science*, 2012, 1–11. <https://doi.org/10.1155/2012/302029>
- Stehfest, H. (1970). Algorithm 368 - Numerical inversion of Laplace Transforms. In *Communications of the ACM* (vol. 13, n. 1, pp. 47–49).
- Van Bree, I., De Meulenaer, B., Samapundo, S., Vermeulen, A., Ragaert, P., Maes, K. C., De Baets, B., & Devlieghere, F. (2010). Predicting the headspace oxygen level due to oxygen permeation across multilayer polymer packaging materials: A practical software simulation tool. *Innovative Food Science and Emerging Technologies*, 11, 511–519.
<https://doi.org/10.1016/j.ifset.2010.01.007>
- Wani, A. A., Singh, P., & Langowski, H. C. (2014). Food Technologies: Packaging. *Encyclopedia of Food Safety*, 3, 211–218. <https://doi.org/10.1016/B978-0-12-378612-8.00273-0>

ANEXO – Review Article: Applications and oxygen transfer models in active multilayer food packaging: a theoretical review

Rubia Viana Batista^{1,2}; Wanderson Gonçalves Wanzeller^{1,2}; Loong-Tak Lim³; Ernesto Quast¹; Vânia Zanella Pinto¹; Vivian Machado de Menezes^{1,2*}

¹Food Engineering, Graduate Program of Food Science and Technology, Universidade Federal da Fronteira Sul, UFFS, Campus Laranjeiras do Sul, BR 158 km 405, Laranjeiras do Sul, PR, Brazil.

² Research Group of Theoretical Modeling and Simulations of Physical Systems, Universidade Federal da Fronteira Sul, UFFS, Campus Laranjeiras do Sul, BR 158 km 405, Laranjeiras do Sul, PR, Brazil.

³Department of Food Science, University of Guelph, Guelph, Ontario N1G2W1, Canada.

E-mail:

Rubia Viana Batista: rubiavianabatista@gmail.com

Wanderson Gonçalves Wanzeller: wanderson@uffs.edu.br

Loong-Tak Lim: llim@uoguelph.ca

Ernesto Quast: ernesto.quast@uffs.edu.br

Vania Zanella Pinto: vania_vzp@hotmail.com

Vivian Machado de Menezes: demenezes.vivian@gmail.com

*Corresponding author: demenezes.vivian@gmail.com, Phone: +55 (42) 3635-8694.

ABSTRACT

Background: Active packaging systems are being used to extend shelf life and preserve the physical, chemical, microbiology, and nutritional quality of food products. In particular, such systems are applied to avoid O₂ ingress that can lead to the deterioration of many food products. To overcome this issue, oxygen scavenging technologies are being deployed to reduce the oxygen exposure on food products and thereby extending their shelf-life.

Scope and approach: Oxygen barrier packaging systems are based on exploiting composite materials to reduce the overall O₂ permeability of the package, such as by incorporating oxygen scavengers. Many mathematical models that simulates the oxygen transport in polymeric materials with oxygen absorbers have been developed to predict the barrier performance under various end-use conditions. This review provides a comprehensive overview on various oxygen absorber systems used in active food packaging and summarizes the mathematical models that simulate the transport and absorption of oxygen in different polymer films.

Key findings and conclusion: In this review, barrier properties of typical thermoplastics food packaging are summarized, as well as commercially available products and patent literature. Numeric methods are reviewed to demonstrate the behavior of O₂ transport in monolayer and multilayer films. The mathematical model's simulations report properly the O₂ behavior at the specific polymeric materials and absorber systems studies.

PRACTICAL APPLICATIONS

The food industry relies on various technologies to protect food products from deleterious conditions. Many food products are sensitive to oxygen that can promote rancidity, growth of aerobic microorganisms, browning, depletion of vitamins, and flavor losses. The incorporation of oxygen scavengers in the packaging structure can eliminate or reduce these undesirable deteriorative reactions to acceptable levels to meet consumers requirements. To this end, mathematical models are useful to predict the behavior of active packaging materials to reduce product development time and cost.

KEYWORDS: Food packaging; Oxygen scavenging; Mathematical modeling; Multilayer system; Active packing; Polymer materials

A1. INTRODUCTION

Food industry selects a packaging system according to the food product requirements in providing optimal containment and protection from external and internal deleterious factors, such as microorganisms, oxygen, water vapor, light, mechanical shock, and others (Restuccia et al., 2015; Wani et al., 2014). Also, packaging provides essential product information to consumers and facilitates product sales through advertisement, in addition to enhancing end-use convenience (Mihindukulasuriya & Lim, 2014). An optimal packaging design must take factors like such as sealability, polymer processability, printability, strength, cost-effectiveness, sustainability, legal requirements, among others (Deshwal et al., 2019; Mihindukulasuriya & Lim, 2014). Moreover, the package should be adaptable to the specific type of food it contains, by considering the product's inherent susceptibility to heat, oxygen, mechanical perturbation (Akelah, 2013). Typical materials for food packaging applications are those derived from glass, metals (aluminum, tinplate, tin-free steel), paper/paperboards, and thermoplastics polymers (Akelah, 2013; Marsh & Bugusu, 2007).

Thermoplastic polymers are commonly used for food packaging due to their lightweight, transparency, cost effective, and easy of processing. Moreover, polymers provide a wide range of thermal/mechanical/barrier properties to fulfill the principal functions of package, i.e., containment, protection, communication, convenience (Geueke et al., 2018; Kirwan et al., 2011; Silvestre et al., 2011). Plastic packaging can be monolayer made up of single polymer, such as poly(ethylene terephthalate) (PET), high density polyethylene (HDPE), low density polyethylene (LDPE), polypropylene (PP), polyvinyl-chloride (PVC), polyvinylidene chloride (PVdC), ethylene vinyl alcohol copolymer (EVOH), polyamides (PA), and polystyrene (PS). On the other hand, multilayer structures contain more than one type of plastic layers produced by coextrusion, blending, lamination, and coating to achieve material properties that cannot be provided by one polymer alone (Geueke et al., 2018; Kirwan et al., 2011). In addition, active compounds may be incorporated to further enhance the material properties of the composite structure (Zhang et al., 2015; Carrizo et al., 2016; Moshe Dvir et al., 2019).

A great attention on oxygen scavenging or reducing into food packaging is due to its important rule on aerobic spoiling and deteriorate microorganisms, enzymatic and oxidation reactions (J. S. Lee et al., 2018), as well as, enables breathing and ethylene

production of fruits and vegetables (Mangaraj et al., 2009) and insects growing (Bodbodak & Rafiee, 2016). Food sensory attributes are affected by the oxygen presence, that can generate strange odors and flavors, because the reactions such as lipid oxidation (Jongberg et al., 2014). Color is highly affected by chlorophylls and carotenes oxidation, and some vitamins, such as A, C, and E, also are oxidized under oxygen atmosphere (Bodbodak & Rafiee, 2016). Active packaging systems are composed by mechanisms that can be activated by intrinsic/extrinsic factors to provide desirable action for extending shelf-life, improving the quality, and/or safety to the food products. Examples of active packaging systems include oxygen scavengers, ethylene scavengers, odor absorbers/releasers, antimicrobials, antioxidants, and others (Galotto et al., 2015; Han et al., 2018; Schaefer & Cheung, 2018; Wyrwa & Barska, 2017; Lim, 2011). Often these systems are based on the incorporation of active compounds or nanomaterials into the packaging structure to improve barrier properties against gases and vapors (e.g., oxygen, carbon dioxide, water, ethylene) (Andersson et al., 2002; Dey & Neogi, 2019; Foltynowicz, 2018; Hutter et al., 2016). For reduced oxygen modified atmosphere applications, composite packaging structures incorporated with oxygen scavenging compound during polymer processing are commonly used, to remove/reduce oxygen in package headspace (Ahn et al., 2016; Akelah, 2013; S. Y. Lee et al., 2015; Summerfield et al., 2012; Wołosiak-Hnat et al., 2019). Other approaches involving oxygen scavengers use sachets that are packaged with the product (Hsiao Sung Non-Oxygen Chemical Co. Ltd, 2020; Mitsubishi Gas Chemical, 2020) or low profile labels that are adhered to the inside of package structure (Cruz-Romero & Kerry, 2016; Labels & Labeling, 2003). Many of them are commercially available being the sachets and labels based on iron and ferrous oxide powders which are very effective in scavenging oxygen (Han et al., 2018). Other approach involve the use of enzymatic O₂ scavenger based on glucose oxidase or ethanol oxidase enzymes that are commercially less common (Cruz-Romero & Kerry, 2016).

The deployment of oxygen scavenger in food packaging is often based on trial-and-error approach, which can be costly and time consuming. Thus, to predict the performance of the active packaging system, the use of mathematical models to simulate oxygen transport can be useful (Carranza et al., 2010, 2012; Di Maio, Marra, Bedane, et al., 2017; Ferrari et al., 2009). These models facilitate the systematic study of different materials and multilayer configurations, reducing research time and increasing the accuracy of prediction. This paper provides a comprehensive review of the oxygen

absorber systems used in food packaging applications, focusing on mathematical models that simulate the transport and absorption of oxygen in different polymer films.

A2 OXYGEN BARRIER PACKAGES

A2.1 POLYMER MATERIALS FOR FOOD PACKAGING

Polymers for food packaging are thermoplastics which have the ability to soften and flow by increasing heat and pressure and solidify into defined shapes when cooled, being a reversible process that can be repeated. Because of this they can be injection molded, extruded, or formed by other molding techniques. Whereas thermosets undergo molecular crosslinking after “setting” and cannot be reshaped by melting, at elevated temperature, thermosets undergo structural degradation, rather than melting (Callister Jr & Rethwisch, 2018).

The majority of polymers used in food packaging which must be stable and not undergo undesirable physical and chemical changes during processing and storage. Table 1 summarizes the most used thermoplastics materials for packaging, its properties and food applications. For example, thermoplastic packaging must withstand freezing (-25 °C) condition for frozen product (e.g., ice cream, frozen vegetables and meats) packaged in LPDE, PP, and PET. Other packaging must hold up to sterilization temperatures (121 °C), such as steamed vegetables in bags and vacuum films, such as PP, PET, EVOH, PA6,6. Packages for microwavable/ovenable ready-to eat frozen products not only must withstand freezing condition, but also tolerate heating microwave and oven heating condition which can reach as high as 220 °C (e.g. PET, PA 6,6) (Bhunia et al., 2013; Kirwan et al., 2011).

In food packaging applications where barrier properties are required, multilayer films are often being used in accordance with each product needs. Multilayer structures can be configured to exhibit barrier and mechanical properties, in addition to considering the heat sealability, adhesion, and printability, as well as meet food contact safety requirements. When optimized, multilayer films can reduce the total amount of material used during manufacturing process and hence the costs reduction (Anukiruthika et al., 2020; Crippa et al., 2007; Dave et al., 2017; Di Maio, Marra, Bedane, et al., 2017; Robertson, 2013). The multilayer system can also use recycled polymers as an inner layer, so the outer polymer layers act as functional barriers with respect to the migration of

compounds from the recycled material to the packaged food (Lagarón, 2011; Mastromatteo & Del Nobile, 2011).

However, even using fewer materials, co-extruded and laminated multilayers sheets are difficult to recycle, since they combine two or more materials, with different processing properties. Other factors that make it difficult to recycle are the lack of multilayer film identification systems (for example, PA / PE, PET / PE, etc.); an adequate solid urban waste collection and management, avoiding the disposal with different materials (Tartakowski, 2010). The recycling multilayers involves steps that separate each layer, that can be physical or chemical process, or both. It can still be carried out by mixing the materials without separating layers, but most mixtures have poor mechanical properties. These materials recycling technologies available have limitations in terms of energy requirements, recycling rates, gas emissions, and high cost, such as pyrolysis, gasification and chemolysis and others process (Anukiruthika et al., 2020). Some studies provide promising results for sustainable techniques, in order to support the superior functionality of the multilayer packaging systems (Mumladze et al., 2018; Samorì et al., 2017; Tatariants et al., 2017).

Table A1 Thermoplastic materials for food packaging and its applications.

Polymer and its classification	Physical properties	Chemical, mechanical, and other properties	Barrier properties; Oxygen Permeation (OP) 23°C; 0%RH (cc.mil/m ² .datm)	Food applications
Low-density polyethylene (LDPE) Structural polymer	Density: 910-925 kg m ⁻³ ; low-regular transparency, low crystallinity, working temperature -50 to 80°C	Good resistance traction and perforation, flexible, heat sealable, printable. Resistance to chemicals and low permeability oil and grease	High moisture barrier; very low gases (O ₂ , N ₂ , CO ₂) barrier; OP: 6500-7800	Frozen food bags, coating, multilayers films (internal layer), flexible lids, injectable bottles (syrup, mayonnaise, ketchup, mustard), blisters and seals
Linear low-density polyethylene (LLDPE) Structural polymer	Density: 910-940 kg m ⁻³ ; low-regular transparency, low crystallinity, working temperature -30 to 100°C	Tough, extensible, good resistance to grease, and good sealing properties	High moisture barrier and very low gases barrier. OP: 6500-7800	Stretch, cling wrap, heat sealant coating.
High-density polyethylene (HDPE) Structural polymer	Density: 945-967 kg m ⁻³ , low transparency, high crystallinity, working temperature: -40 to 120°C	Good resistance mechanical, median resistance to grease and chemical products, good sealing properties and easy to process and form	Very high moisture barrier and very low gases barrier; OP:1600-2300	Margarine jars, buckets, rotomolded pallets, boxes, bottle crates, drumsticks, garbage bags, and retail bags, lids
Polypropylene (PP) Structural polymer	Density: 900-915 kg m ⁻³ ; regular transparency, low crystallinity, working temperature: -40 to 120°C; melting temperature: 160°C	Variable mechanical resistance, moderately rigid, Strong and good resistance to chemicals and grease	High moisture barrier and low gases barrier	Margarine jars, buckets, pallets, boxes, crates, drums, bags and sacks, heated packaging and microwaves, films.
Polyethylene terephthalate (PET, PETE) Structural polymer	Density: 1380-1410 kg m ⁻³ ; high transparency, low crystallinity, melting temperature -60 to 220°C	High breaking strength and good resistance to grease and chemical products (acids and solvents)	Good moisture and gases barrier, high barrier to odors and contaminants; OP:55-70	Bottles, pots and tubes, semi-rigid sheets (trays and blisters) and oriented thin films (bags and packaging for snacks)
Polyethylene naphthalate (PEN) Barrier polymer	Density: 1360 kg m ⁻³ ; high transparency; low or high working temperatures	High mechanical, chemical and hydrolytic resistance, high thermal and thermo oxidative performance	Good water vapor and gases barrier, light UV barrier	Ready to heat food, beer, and wine bottles to preserve flavor
Polyvinyl chloride unplasticized (PVC-U) Structural polymer	Density: 1350-1450 kg m ⁻³ ; high transparency; melting temperature -2 to 80°C	Strong, stiff ductile, resistance to chemicals, and stable electrical properties. Good resistance to oil and grease	Good gases barrier and moisture barrier media	Bottles and films. Has limitation for use in food
Polyvinylidene chloride or Polyvinylidene dichloride (PVdC) Barrier polymer	Density: 1600-1700 kg m ⁻³ ; high transparency; melting temperature: -20 to 130°C	Strong, stiff ductile, resistance to chemicals, oil, and grease, stable electrical properties	High gases and water vapor barrier; OP: 1.2-14	Poultry, cured meats, cheese, tea, coffee, snacks, and confectionery. Hot products and modified atmosphere storage
Polystyrene (PS) Structural polymer	Density: 1030-1100 kg m ⁻³ ; very high transparency; melting temperature: -20 to 90°C	Low resistance to impact/perforation. Low resistance to oil and grease.	Low gases and moisture barrier; OP: 5425	Packaging for eggs, disposable practical utensils, cups, plates, bottles, and meat trays
Ethylene vinyl alcohol (EVA) hydrolyzed (EVOH) Barrier polymer	Density: 1140 – 1210 kg m ⁻³ high transparency; working temperature; -20 to 150°C	Rigid, strong, and high resistance to oil and greases	Excellent gas barrier, high moisture barrier; OP: 0.3 (32mol% ethylene) OP: 1.2 (44mol% ethylene)	Coextruded films
Polyamide (PA, PA 6, Nylon) Structural and barrier polymer	Density: 1130 – 1160 kg m ⁻³ ; high transparency; working temperature: -20 to 150°C	Excellent mechanical resistance to traction and impact/perforation; good resistance to grease and some chemical compounds	High gas barrier and low moisture barrier; OP: 40-60	Ready to heat packaging

Source: (Bhunia et al., 2013; Callister Jr & Rethwisch, 2018; Lechevalier, 2016; Morris, 2017; Shin & Selke, 2014; Wani et al., 2014)

A2.2 OXYGEN BARRIERS SYSTEMS AND MECHANISMS

Permeation phenomena is governed by diffusion and solubility of the permeant molecules, which are strongly affected by the physical properties of the material, the penetrant, and the conditions in which they are found (Lechevalier, 2016). Among the factors associated with the polymers, its specific molecular structures affect barrier properties, as highly polar polymers are excellent gas barrier, while, a non-polar hydrocarbon, have poor gas barrier properties. Other factor that affect the way that permeate molecules move through the free volume or voids of the polymers are molecular packing in the amorphous phase, as well as the molecular orientation can increase packing density and thus decrease the permeability. Crystallinity regions are impenetrable in most semicrystalline polymer, therefore, an increase in crystallinity can reduce permeability.

The thickness of the material must also be considered when assessing its permeability, as increasing the thickness, permeability proportional inversely decreases. The permeability coefficient may or not also vary with pressure. Permeability is pressure dependent in cases where the interaction between the permeant and the polymer, increasing as there is a pressure increase. The gas permeability of a specific polymer permeate system may increase with increase in temperature, as it is directly proportional related to the diffusion and solubility coefficients (Arrhenius relationship). Sorption of organic molecules in polymeric films, present in food such as flavor, aroma and pigments molecules, can increase O₂ permeability by two to four times, because it act as plasticizing agents, increase in the free volume and allowed transfer O₂. The use of plasticizers is ordinary and helps to maintain the flexibility of the plastics, however, due to the increasing the space between the polymer chains, its addition causes an increase in the permeability (McKeen, 2012a, 2012b; Robertson, 2016).

The copolymerization can improve the barrier properties of polymers. It is based on combining two or more polymers with different characteristics, in which one or more homopolymers are linked in a chain, forming a single copolymer (alternating, random, block or by grafting). Also, polymers blend can be carried out, by two or more polymers melting to form a mixture that will have the properties of both polymers. Other ways to improve the barrier properties are to use multilayer, metallized, coated films or composite materials (McKeen, 2012b).

The oxygen permeability of the polymers is affected by temperature, due to the phase change in the polymer structure, as well as, at higher levels of relative humidity (RH), the oxygen permeability increase due to the polar groups from the polymers structure (Turan et al., 2017). The phenomenon of diffusion is dependent on the thickness of polymer (Fick's Law), so the thickness also affects oxygen permeability, and in the case of multilayer films, the oxygen permeability rate is a function of each different layers (Crippa et al., 2007). Studies have shown that the polymers oxygen permeability can be reduced with the active oxygen scavengers (OS) incorporation, micro or nanosized, in the multilayer materials (Busolo & Lagaron, 2012; Foltynowicz, 2018). It was demonstrated the effectiveness in decreasing the oxygen permeation rate in the inert layer of a polymeric film composed of three layers, in which the intermediate layer contained oxygen scavenging compared to a single active layer (Apicella et al., 2018a).

A2.2.1 Oxygen scavengers (OS)

OS are the most used active packaging systems for food products. Its working principle is based on the oxidation of the scavenging agents by the oxygen consume (Shin & Selke, 2014). Different systems have been tested and developed based on the OS inclusion into the films, and as sachets, using antioxidant, sulfite-based, enzymes, iron powder, ascorbic acid, unsaturated fatty acids, among others (Brody et al., 2001; Galdi & Incarnato, 2011; Labuza & Breene, 1989). Table 2 summarizes the oxygen scavenging systems for food package uses, including experimental and commercial products as well as patents and their applications.

The antioxidants with potential oxygen scavenger, α -tocopherol has shown good results in active packaging systems, as it is a natural free radical scavenger (Table 2). It is usually combined with a catalyst (transition metal) that reacts with oxygen, and later, there is a scavenging of free radicals by the α -tocopherol (Byun et al., 2011). α -tocopherol was encapsulated in microparticles of poli (lactic) acid (PLA), and resulted in an effective capacity and rate of oxygen scavenging (Scarfato et al., 2017).

A nonmetallic oxygen scavenger sulfite-based, using sodium metabisulfite, has antioxidant activity and was used for Kimchi packaging, a Korean traditional fermented vegetable food. The developed OS inhibited oxygen-mediated Kimchi deterioration, without affecting the vegetable fermentation. This OS demonstrated the potential for active packaging development, decreasing quality-degradation due to oxygen in Kimchi.

The use of sulfite-based systems is suitable for food that, after packaging, pass through metal detectors (J. S. Lee et al., 2018).

Systems based in palladium can be used in modified atmosphere packaging- MAP (2 vol.% O₂, 5 vol.% H₂, 93 vol.% N₂) eliminating the residual oxygen by oxidation of hydrogen into water. It was shown that the optimal palladium layer thickness for OS films lies between 0.7 and 3.4 nm (Yildirim et al., 2015). The palladium-based system demonstrated the potential to extend shelf-life and improve the quality of oxygen-sensitive foods packaged in MAP (Röcker et al., 2016; Yildirim et al., 2015). However, OS based on palladium as catalytic system is inactivated by sulfur-containing compounds (Röcker et al., 2016; Yildirim et al., 2015), which cannot be used for meat and protein products.

Enzyme systems are also described in literature with potential oxygen scavenging for food packaging. Barley oxalate oxidase was immobilized in a latex polymer matrix (styrene-butadiene co-polymer) to act as an oxygen scavenger. Its co-immobilization with catalase in films is also an efficient approach to degrade the hydrogen peroxide produced in a reaction catalyzed by an oxidase (Table 2). Oxalate oxidase in active packaging can be used as part of an oxygen scavenging system or as an agent to remove unwanted oxalic acid from food and drinks (Winestrard et al., 2013).

Sachets with iron powder are the most used in the food industry, reducing the oxygen concentration in the headspace to less than 0.01% (Shin & Selke, 2014). In general, these scavengers are based on the principle of iron oxidation in the presence of water (Cruz et al., 2012). The iron powder base OS and different additives, activated with relative humidity above 70%, recommend to cold food (Shelfplus® 2400 and Shelfplus® 2500), currently owned by Albis Plastic, were studied to improve frozen sausage packages. This OS incorporated in low oxygen barrier polymer (EVA) increased the oxygen scavenging on co-extruded film (PE/Active Layer (Shelfplus® 2500:EVA)), resulting in high oxygen consumption in less time, increasing the product protection by no free-oxygen into the package (Gibis & Rieblinger, 2011).

Another technique that demonstrates a high oxygen scavenging capacity includes the oxidation of unsaturated hydrocarbons (Table 2), which has the advantage the use for dry food packing. 1,4-polybutadiene is one of the most commonly used hydrocarbons for oxygen scavenging (Li et al., 2012). The commercial oxygen scavenger Amosorb™ 4020E (AMS – ColorMatrix™ Europe) was wildly studied. It is a copolyester-based

polymer (Polybutadiene + PET) designed for rigid PET containers and the OS mechanism is auto activated by moisture.

Four configurations of PET films containing three-layers were produced by co-extrusion, containing AmosorbTM DFC 4020E as the OS into an intermediate layer. The configurations were based on thicknesses of the inert/active/inert layers: (i) 6.75 / 23.5 / 6.75 μ m; (ii) 6.75 / 13.5 / 6.75 μ m; (iii) 11.75 / 23.5 / 11.75 μ m; (iv) 11.75 / 13.5 / 11.75 μ m). Single-layer films were also produced to assess the individual contribution of active (25 μ m) and inert (40 μ m) layers (Apicella et al., 2018b). Keeping the thickness of the inert layer constant (6.75 μ m), it was possible to observe an increase in oxygen consumption when the active layer thickness was extended (e.g., configuration ii: 13.5 μ m → i: 23.5 μ m). When the thickness of the active layer was kept constant (13.5 μ m) and the inert layer thickness was extended (e.g., configuration ii: 6.75 μ m → iv: 11.75 μ m) there was an increase in the oxygen consumption time. The inert layers of the multilayer films contributed to the deceleration of oxygen permeation when compared to the individual active layer. Due to the presence of the second phase in the polymeric matrix of the active films, there was a decrease in the mechanical properties (elastic modules, stress at break, strain at break) when compared to monolayer PET; however, it was recovered by the outer layer of the pure inert polymer, in multilayer samples (Apicella et al., 2018a, 2018b).

The same research group studied a three-layer active film (PET/PET: AmosorbTM 4020/PET). Fresh broccoli sprouts were pack in these bags (10cm*15cm) with thickness varying at each layer, and storage at 5°C, for 15 days (Di Maio, Marra, Apicella, et al., 2017). This study indicated that the OS autoactivates AmosorbTM 4020 was efficient to reduce the vegetable senescence caused by oxygen-dependent oxidation reactions.

Table A2 Oxygen scavenging systems for food package uses.

Base systems	Compounds	Mecanisms	Reactions	Patent and companies	Packaging systems and commercial products	Reference
Antioxidants	Ascorbic acid + (Iron or Zinc)	Ascorbic acid (AH_2) oxidation to dehydroascorbic acid (A) or in metal-ascorbate complex formed in case of catalyzed reaction	$AH_2 \xrightleftharpoons{k1} HA^- + H^+$ $HA^- + M^{n+} \xrightleftharpoons{k2} MHA^{(n-1)+}$ $MHA^{(n-1)+} + O_2 \xrightleftharpoons{k3} MHA(O_2)^{(n-1)+}$ $MHA(O_2)^{(n-1)+} \xrightleftharpoons{k4} MH\dot{A}(O_2)^{(n-1)+}$ $MH\dot{A}(O_2)^{(n-1)+} \rightarrow H\dot{A}^- + M^{n+} + \dot{O}_2$ $H\dot{A}^- + M^{n+} \rightarrow A + M^{(n-1)+}$ $H\dot{A}^- + O^2 \rightarrow A + \dot{O}_2^-$ $M^{(n-1)+} + H\dot{O}_2 + H^+ \rightarrow M^{n+} + H_2O_2$	-	Extrusion with LLDPE	(Matche et al., 2011)
	α -tocopherol	Free-radical scavenging activity	Not provided	-	Encapsulated in PLA microparticles	(Scarfato et al., 2017)
	α -tocopherol + Iron chloride (II)	A catalyst (transition metal) that reacts with oxygen and the followed occurs the free radical scavenging by tocopherol.	$O_2 + Fe(II) \rightarrow O_2^\cdot + Fe(III)$ $O_2^\cdot + TocH \rightarrow Toc^\cdot + HO_2^\cdot$ $HO_2^\cdot + TocH \rightarrow H_2O_2 + Toc^\cdot$ $Fe(II) + H_2O_2 \rightarrow Fe(III) + HO^\cdot + OH^-$ $O_2^\cdot + HO^\cdot \rightarrow O_2^\cdot + OH$ $O_2^\cdot + TocH \rightarrow Tocopherylquinine$ $Fe(III) + H_2O_2 \rightarrow Fe(II) + O_2^\cdot + H^+$	-	In retortable plastic cups with 3% EVOH barrier with lid of PET/nylon/aluminium foil/cast PP	(Byun et al., 2011)
Sulfites	Sodium metabisulfite	Not provided	Not provided	-	Sachet HDPE	(J. S. Lee et al., 2018)
Enzymes	Glucose oxidase + catalase	Reaction of O_2 with glucose in presence of water catalyzed by glucose oxidase, forming gluconic acid and hydrogen peroxide, the latter being degraded by catalase	$2 \text{ glucose} + 2O_2 + H_2O \xrightarrow{GOx} D - \text{glucono} - 2 \text{ gluconic acid} + 2H_2O_2$ $2H_2O_2 \xrightarrow{\text{cat}} 2H_2O + O_2$	Labuza & Breene (1989)	PP and PE such as substrates for immobilizing enzymes	(Andersson et al., 2002)
	Oxalate oxidase + catalase	Catalase degrades the hydrogen peroxide produced in the reaction catalyzed by oxalate oxidase	$HOOC \cdot COO^- + H^+ + O_2 \xrightarrow{OOx} 2CO_2 + H_2O_2$ $H_2O_2 \xrightarrow{\text{cat}} H_2O + \left(\frac{1}{2}\right) O_2$	-	Immobilized in a latex polymer matrix (styrene-butadiene copolymer)	(Winestrand et al., 2013)
	Laccase (EC 1.10.3.2) + lignosulfonates	Copper-containing laccase catalyzes a one-electron oxidation of phenolic hydroxyl groups to phenoxy radicals, while oxygen is reduced to water	$4PhOH + O_2 \xrightarrow{\text{laccase}} 4 PhO \cdot + 2H_2O$	-	Included in coating colors and incorporation in latex-based or starch-based film	(Johansson et al., 2012)
Unsaturated Hydrocarbons	10% unhydrogenated hydroxyl-terminated polybutadiene oligomer + 90% PET	Oxidation of unsaturated hydrocarbons of the polybutadiene, activated with moisture	Not provided	Tibbitt et al., 2007 Commercial brand ColorMatrix®	ColorMatrix® Amosorb®4020 Low-Hazer, ColorMatrix™ Amosorb™ Oxygen Scavenger for PET,	(Di Maio, Marra, Bedane, et al., 2017; PolyOne, 2020; Tibbitt et al., 2007)

					ColorMatrix™ Amosorb™ SolO2 CO2 Barrier and Oxygen Scavenger for PET and ColorMatrix™ HyGuard™ Oxygen Scavenger for PET	
	Residues of terephthalic acid, ethylene glycol and isophthalic acid +Transition metals (Li, Al, P, Sb, Zn)	Oxidation of unsaturated hydrocarbons in the presence of transition metal	Not provided	Stewart &Armentrout (2010)	PET Film	(Dey & Neogi, 2019)
	1,4-polybutadiene + cobalt neodecanoate	Oxidation of unsaturated hydrocarbons in the presence of transition metal	$O_2 + RH \rightarrow ROOH$ $Co^{2+} + ROOH \rightarrow Co^{3+} + OH^- + RO$ $Co^{3+} + ROOH \rightarrow Co^{2+} + OH^- + ROO^-$	-	Combined use of polybutadiene polymer with cobalt neodecanoate prepared by casting	(Li et al., 2012)
	1,2- polybutadiene + Transition metal salt + photosensitizer	Polymer oxidation, catalyzed by the transition metal salt and activated by UV light	Not provided	Sealed Air® - Cryovac®	Freshness Plus Active Barrier OS Films- Cryovac® OS2000	(Cooksey, 2010; Fang et al., 2017; SealedAir, 2020)
	Iron and nano-iron based	Oxidation in presence of water or Lewis acids or anhydrous environment	$Fe \rightarrow Fe^{2+} + 2e^-$ $\frac{1}{2} O_2 + H_2O + 2e^- \rightarrow 2OH^-$ $Fe^{2+} + 2OH^- \rightarrow Fe(OH)_2$ $Fe(OH)_2 + \frac{1}{4} O_2 + \frac{1}{2} H_2O \rightarrow Fe(OH)_3$	Foltynowicz, 2014	Matrix Silicon (food grade silicone moulding rubber), PA6,6, PVA and PE	(Dey & Neogi, 2019)
Metal and metal ions	Iron based	Not provided	Not provided	Multisorb Filtration Group	Self-Adhesive FreshMax® Fresh Plus® Film-Based (LLDPE, PP, EVA, PET) FreshPax® Packets	(Multisorb Filtration Group, 2020)
	Iron based	Not provided	Not provided	Mitsubishi Gas Chemical Company	FreshCard® Sachet Ageless® Ageless OMAC Film	(Mitsubishi Gas Chemical, 2020)
	Iron/Organic based	Not provided	Not provided	Dutch Desiccants Company	Sachet ATCO®	(Dutch Dessicants Company, 2020)
		Not provided	Not provided	Henkel Corporation	DARAFORM®, CELOX®, Bottle cap beer, juice, tea, sport drinks	(Henkel AG & Co., 2017)
	Iron oxide and zeolite	Not provided	Not provided	Hsiao Sung Non-Oxygen Chemical Co., Ltd.	Sachet O-Buster®	(Hsiao Sung Non-Oxygen Chemical Co. Ltd, 2020)

	Iron+(FeCl ₃ /AlCl ₃)	Oxidation metal or metal alloy with a hydrolysable halogen compound as the activating	Not provided	(Rollick, 2010)	Incorporation into PET film	(Dey & Neogi, 2019)
	Palladium	Eliminating the residual oxygen by oxidation of hydrogen into water	Not provided	-	Deposited in PET/SiO _x film	(Hutter et al., 2016; Yildirim et al., 2015)
	Iron-based and other additives	Oxidation of iron powder activated at a relative humidity above 70%	Not provided	Albis Plastic	Shelfplus™ O ₂ –extrusion with PE-based resin for films compatible with PP e PE, PA e EVA	(Albis Plastic, 2020; Gibis & Rieblinger, 2011)
Others	Does not reveal the composition	Activated with moisture	Not provided	Clariant International Ltd	Sachets Oxy-guard™ Oxygen Scavengers and Oxy-guard™ Case Ready Meat Oxygen Absorber	(Clariant Internation Ltd, 2018)

A3. MATHEMATICAL MODELING AND SIMULATION OF OXYGEN-SCAVENGING POLYMERIC SYSTEMS

A3.1 DIFFUSION THEORY

The permeation mechanism through a polymer film occurs in three steps: (i) sorption of a gas on the polymer surface; (ii) diffusion of gas through the polymer; (iii) gas desorption on the other side of the material (Belay et al., 2016; Mangaraj et al., 2009; Morris, 2017). Permeation is based on Fick's law of diffusion and Henry's law of solubilization that considers the relative sizes of the molecules and their sizes compared to the free volume in the solid material. Permeability is generally being used as an index for quantitative assessment of the barrier properties of a plastic material (McKeen, 2012a; Robertson, 2016; Siracusa, 2012). The first and third steps of permeation depend on the permeate solubility in the polymer, which is defined as the ratio of the equilibrium concentration of the penetrant in the polymer to its partial pressure in the gas phase (Henry's Law) (Lagarón, 2011), while the diffusion process in the material is determined by the first Fick's Law (Crank & Park, 1968):

$$F = -D * \frac{dC}{dx} \quad (A1)$$

where F is transfer rate per unit area of the given section, D is diffusion coefficient of the gas in a polymeric matrix, C is the concentration of the diffused substance, x is coordinated one-dimensional measured space in the polymeric material section. Fick's first law describes the diffusion of a gas or vapor through the polymer at a steady state. Fick's second law can be derived from Fick's first law (A1) as follows:

$$\frac{\partial C}{\partial t} + \nabla F = R \quad (A2)$$

where: t is the processing time and R is the chemical reaction involved, i.e., permeant molecules being generated or consumed during the process. In the absence of any chemical reactions and considering the flow in only one direction (x), Fick's second law describes the diffusion in a non-stationary state, i.e., the solute concentration gradient is a function of time (Lagarón, 2011):

$$\frac{\partial C}{\partial t} = D * \frac{\partial^2 C}{\partial x^2}. \quad (A3)$$

Barrier properties in polymers are associated with their inherent ability to enable the exchange of low molecular weight substances through a mass-transport process like permeation (Lagarón, 2011). The properties of the permeating species and polymers, as well as degree of interaction and the environmental conditions, will determine the rate at which a permeant passes through a polymeric material. Diffusion of permeant molecules by and large takes place in the amorphous domains of the polymer matrices. Crystalline structures are considered impermeable to permeant molecules due to dense molecular packing (Ashley, 1985; Morris, 2017).

A3.2 ACTIVE POLYMERIC SYSTEMS MODELING

Several studies have proposed mathematical models that describe the oxygen transport in active packaging (Table 3). A method was developed a method to predict the entry of oxygen into packages, in order to optimize the design of multilayer barrier films incorporated with a non-catalytic oxygen scavenger, immobilized inside one of the layers. The transient permeation was evaluated through a two-layer film (reactive/passive), where the ideal design for the time of exhaustion of the oxygen scavenger, that is, the time for which every scavenger of the active layer takes to be consumed, depends on the exposure of the reactive layer to the contents of the package and high levels of environmental oxygen that permeate the passive barrier. The useful life of the oxygen scavenger was reduced when the diffusivity of the reactive layer material was less than that of the passive layer material. Reducing the initial transmission rate requires placing the eliminator inside a layer with the lowest diffusivity of the matrix polymer. Therefore, the choice of the passive and active layers of the films and their thickness depends on the type of oxygen scavenger that will be incorporated in the active layer of the packaging (Solovyov & Goldman, 2006a, 2006b, 2006c).

Table A3 Mathematical models of oxygen transport in active polymeric films.

Oxygen Scavenger	Scavenging characteristics	Polymer matrix	Film characteristics	Method and software	Reference
Noncatalytic oxygen scavenger	Not provided	Passive membrane	Single or two layers (reactive and passive)	Not provided	(Solovyov & Goldman, 2006a, 2006b, 2006c)
Polybutadiene + Metal catalysts	Polymer that oxidizes in the presence of a metal catalyst	PET or PS	Spherical particles of oxygen scavenger polymer co-extruded with PET or PS matrix in a single layer	Explicit finite difference method MATLAB	(Ferrari et al., 2009)
Polybutadiene + Metal catalysts	Polymer that oxidizes in the presence of a metal catalyst	PET or PS	Spherical particles of oxygen scavenger polymer co-extruded with PET or PS matrix in a single layer	Explicit finite difference method MATLAB	(Carranza et al., 2010)
Polybutadiene + Metal catalysts	Polymer that oxidizes in the presence of a metal catalyst	PET or PS	Oxygen scavenger co-extruded with PET or PS matrix in a multilayer (3 for 7 layers interleaving inert and active layer)	Explicit finite difference method MATLAB	(Carranza et al., 2012)
AMOSORB DFC 4020 (PET + unhydrogenated hydroxyl-terminated polybutadiene oligomer)	Co-polymer. It is activated with water	PET	Three layers co-extruded, with inert external layer and active internal layer	COMSOL® 5.0	(Bedane et al., 2015)
AMOSORB DFC 4020 (PET + unhydrogenated hydroxyl-terminated polybutadiene oligomer)	Co-polymer. It is activated with water	PET and PE	Three layers co-extruded, with inert external layer and active internal layer	COMSOL® 5.0	(Di Maio, Marra, Bedane, et al., 2017)

A mathematical model was developed to predict transient mass transfer of oxygen in polymeric films incorporated with spherical particles of an oxygen scavenging polymer (OSP), the polybutadiene, dispersed in PET or PS matrices (Ferrari et al., 2009). The model assumed one-dimensional diffusion, wherein oxygen molecules diffuse through the polymer according to Fick's law and are consumed by the OSP particles and, consequently, its size is reduced, thus reducing the diameter of these OSP particles (Figure A1). The equation for oxygen concentration (A4) and the dynamic equation for the radius of the OSP particle that did not react (A5) with dimensionless parameters, are described below:

$$\frac{\partial \tilde{C}}{\partial \tilde{t}} = \frac{\partial^2 \tilde{C}}{\partial \tilde{x}^2} - 3\phi \frac{(Da)\Delta}{\varepsilon^2 H} \left[\frac{\tilde{a}^2}{1 + (Da)(\tilde{a} - \tilde{a}^2)} \right] \tilde{C} \quad (A4)$$

$$\frac{\partial \tilde{a}}{\partial \tilde{t}} = \begin{cases} -\frac{C_m(0)}{\beta} \frac{(Da)\Delta}{\varepsilon^2 H} \left[\frac{1}{1 + (Da)(\tilde{a} - \tilde{a}^2)} \right] \tilde{C}, & \text{para } \tilde{a} > 0 \\ 0, & \text{para } \tilde{a} = 0 \end{cases} \quad (A5)$$

$$\tilde{t} = t / L^2 / D \quad (A6)$$

$$\tilde{C} = C / C_m \quad (A7)$$

$$\tilde{a} = a / R \quad (A8)$$

$$\tilde{x} = \hat{x}/L \quad (A9)$$

$$\hat{\varepsilon} = R/L \quad (A10)$$

$$\Delta = D_p/D_m \quad (A11)$$

$$H = S_p/S_m \quad (A12)$$

$$Da = k \cdot R / D_p \quad (A13)$$

where: C (mol/cm^3) is the initial concentration of oxygen in the environment, C_m (mol/cm^3) is the concentration of oxygen in the polymeric phase, t (s) is the time of process, L (cm) is film thickness, D (cm^2/s) is diffusion coefficient, \hat{x} (cm) is the one-dimensional coordinate space, a (cm) is the radius of the nucleus that did not react with the OSP particles, R (cm) is the radius of the OSP particle, \emptyset is the volumetric fraction of radius R , D_p (cm^2/s) is the OSP diffusion coefficient, and D_m (cm^2/s) is the diffusion coefficient of polymeric matrix. The parameter β ($mol O_2/cm^3$) is defined as the moles of oxygen consumed per unit volume of the OSP. The partition coefficient is given by H , where S_p ($cm^3/cm^3 \cdot MPa$) is the solubility coefficient of the oxygen in the oxidized polymer and S_m ($cm^3/cm^3 \cdot MPa$) is the effective solubility coefficient. Da is the Damköhler number for an OSP particle, that is, a ratio between a particle time scale and a time scale of the particle reaction, where k ($cm^3/mol \cdot s$) is reaction rate constant. Equations (4) and (5) were numerically solved using an explicit finite difference method. The equations were discretized using a three-point central difference for spatial derivatives and a two-point forward difference for the time derivatives. The numerical solution was developed in MATLAB® for convenient resulting matrix manipulation. When there are no reactive particles in the matrix, the solution is reduced to the classic diffusion in films. The models were found to be in excellent agreement with the analytical solution (Ferrari et al., 2009).

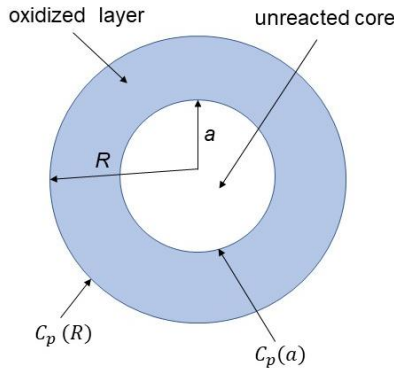


FIGURE A1. Scheme of a spherical particle of an oxygen scavenging polymer (OSP) and particle reduction due to oxidation. C_p is the oxygen concentration in OSP particle. Adapted from (Ferrari et al., 2009).

In a subsequent study by Carranza et al. (2010) a multiscale model for designing reactive polymer mixing barrier materials was developed. The described equations mix spherical particles (OSP), composed of the polybutadiene polymer, with fast or slow reaction rates, in PET or PS polymers considered as a matrix (Figure A2). The oxygen transport through the particle was described by equations (A14) and (A15), where the structure and the numerical solution to derive the analytical design formulas developed for homogeneous reactive membranes by Ferrari et al. (2009) in MATLAB[®] were extended to mixtures of reactive polymers.

$$\frac{\partial C_p}{\partial t} = \frac{D_p}{r^2} \frac{\partial}{\partial r} \left(r^2 \frac{\partial C_p}{\partial r} \right) - k_R n C_p \quad (A14)$$

$$\frac{\partial n}{\partial t} = -\hat{v} k_R n C_p \quad (A15)$$

where: C_p (mol/cm^3) is concentration oxygen in particle, r (cm) is the radial position in spherical coordinates, D_p (cm^2/s) is the diffusion coefficient for oxygen in oxidized scavenging polymer, k_R ($\text{mol}/\text{mol.s}$) is the bulk reaction rate constant for reactive particle, n (mol/cm^3) the concentration of reactive sites and \hat{v} ($\text{mol of } O_2/\text{mol of OSP}$) the stoichiometric constant relating moles of oxygen to moles of reactive sites.

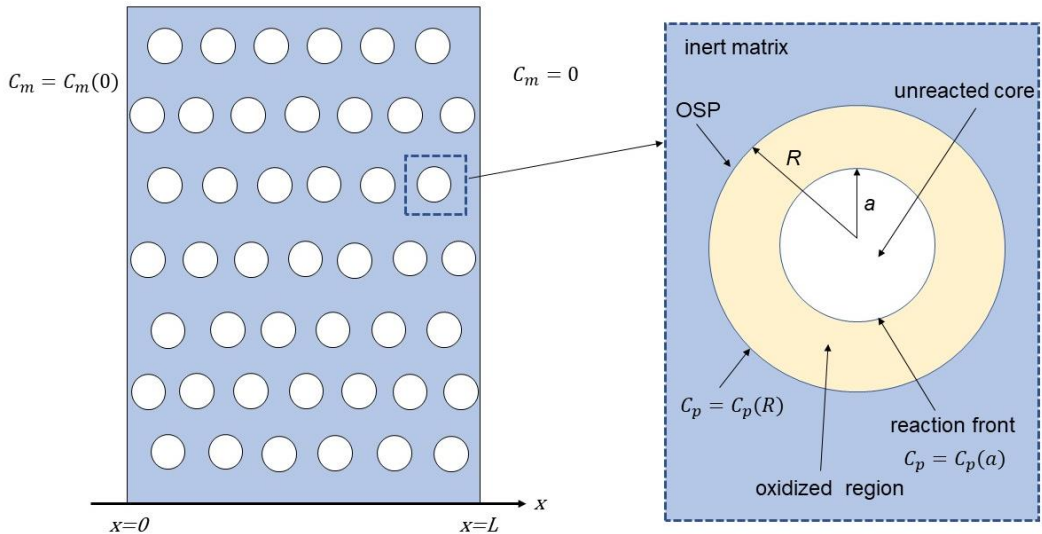


FIGURE A2. Illustration of the polymer blend film and an oxygen scavenging particle behavior in the reaction (Adapted from Carranza et al. (2010)).

It was found that the details of the reaction mechanism within the particles do not affect the functional form of the analytical models, only the values of known or easily determined constants in the predictive equations. The model presented can be widely applied and easily adapted to describe other particle-scale reaction models.

Carranza et al. (2012) considered a model made up of a composite containing OSP particles dispersed in an inert matrix within a multilayer system (Figure A3). The inert layers were made of PET and PS, while polybutadiene was the OSP. The numerical solutions of Equations (A16) and (A17) (with \hat{x} is film thickness) were computed in MATLAB®. Solutions were generated for various layer configurations to understand the effects of changes in barrier properties and multilayer configuration (e.g., number of layers, sequence of polymers) in active systems. The various configurations demonstrated an oxygen barrier property, with systems in which the first layer was inert with better performance than systems in which the first layer was reactive. It was also observed that PET has a greater barrier property than PS, since the latter has greater oxygen diffusivity/solubility. Thus, the selection between polymers blends and multilayer films depends on the properties of the inert matrix and the reactive polymer. Polymers blends are more suitable for diffusion coefficients and/or solubility of the reactive material than diffusion coefficients and/or solubility of the inert matrix, both in terms of time lag and initial flux plateau. Multilayer films were more suitable for reactive materials with small diffusion coefficients and/or solubility in relation to the matrix, when they have higher bulk reaction rates.

$$\frac{\partial C}{\partial t} = \frac{\partial}{\partial \hat{x}} \left(D(\hat{x}) \frac{\partial C}{\partial \hat{x}} \right) - k_R n C \quad (A16)$$

$$\frac{\partial n}{\partial t} = -\hat{v} k_R C n \quad (A17)$$

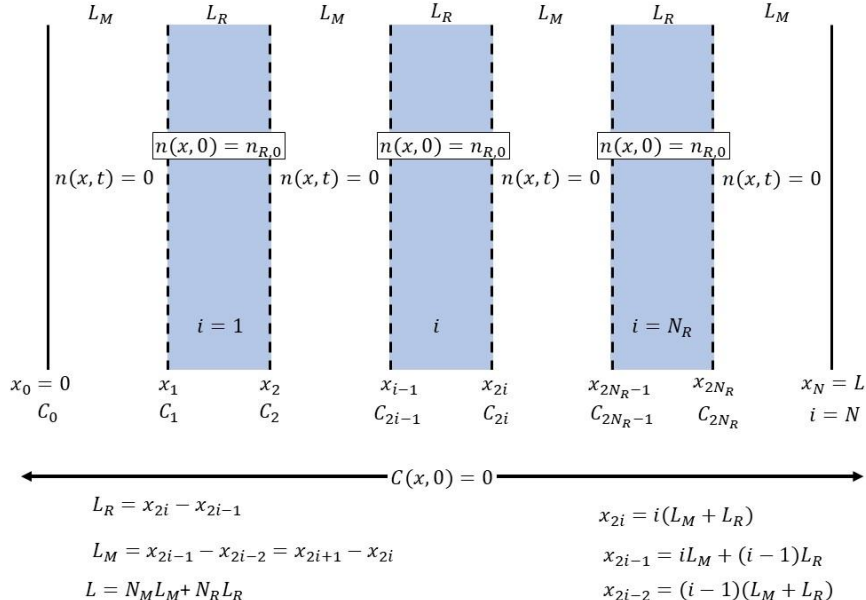


FIGURE A3. Illustration of the polymer barrier formed by inert layers of thickness L_M and reactive layers of thickness L_R , where are the reactive particles. Adapted from (Caranza et al., 2012).

Other authors (Bedane et al., 2015; Di Maio, Marra, Bedane, et al., 2017) also developed mass transfer models to optimize the performance of the oxygen barrier and the configurations of coextruded three-layer structure, containing PET as inert outer layers and PET with a OSP (AMOSORB DFC 4020 - Colormatrix Europe) as the central reactive layer (Figure A4). This central layer was made up of PET polymer loaded with 10% of active OS material (Table A3). The model was developed in COMSOL® 5.0 software. For that, it was necessary to define the mathematical system (equations A18 and A19), as well as the variables and parameters, the system geometry, definition of the different subdomains, initial and boundary conditions, the choice of mesh and adequate post-processing of the results obtained.

$$\frac{\partial C_{oxy}}{\partial t} = D_i \frac{\partial^2 C_{oxy}}{\partial x^2} - k_{bi}^* C_{oxy} \varepsilon \quad (A18)$$

$$\frac{d\varepsilon}{dt} = -\nu k_{bi}^* C_{oxy} \varepsilon \quad (A19)$$

with C_{oxy} (mol/L) the oxygen concentration in polymeric matrix, $D_i(cm^2/s)$ diffusion coefficient layer i , $k_{bi}^*(cm^3/mol.s)$ is the reaction rate constant, ε (mol/L) is number of scavenger moles effectively active and v ($mol de O_2/mol de OSP$) the stoichiometric constant relating moles of oxygen to moles of oxygen scavenging.

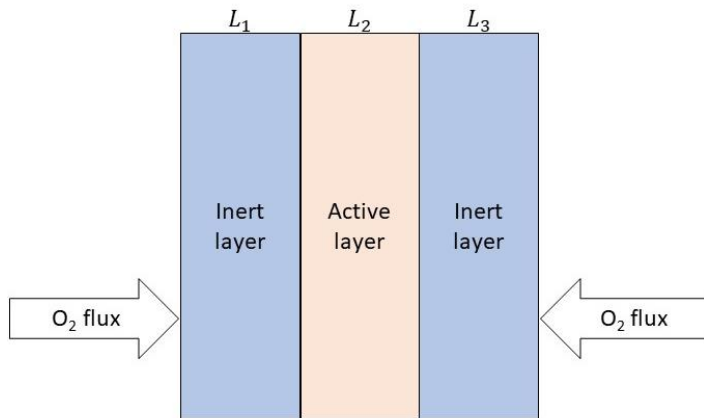


FIGURE A4. Configuration of three-layer film used in the oxygen transfer model.

Adapted from Di Maio, Marra, Bedane, et al. (2017).

The film oxygen absorption activity increased with the thickness of the reactive layer and decreased proportionally with the thickness of the outer layers. Besides, the effect of replacing of one of the inert layers of PET by PE was evaluated, i.e., PET / active layer / PET (ABA) versus PET / active layer / PE (ABC). The model was validated experimentally to predict the behavior of active multilayer films, under different symmetric configurations (ABA) of three layers and could be used to analyze the performance of more general configurations (ABC), when one of the inert layers is replaced by another polymer, such as PE for example (Di Maio, Marra, Apicella, et al., 2017).

One perceives that the studies described in this review depend on extensive mathematical manipulation and specific software for operation. Although they have shown promising results, being validated experimentally. The study of mathematical models that simulate the behavior of oxygen in active multilayer films is still little explored, being a field of work that should better be investigated. The use of simulation tools, to predict the behavior of oxygen in the development of active packaging, would imply the use of less resources in preliminary tests and less generation of plastic waste.

A4. FUTURE TRENDS

The packaging industry has been developing innovative materials and technologies to extend the shelf-life and enhance the safety of food since ever. Due to their interaction, food and packaging must be considered a system, rather than considering them independently. The development of mathematical models that simulate the interaction between environment-packaging-food can be useful in reducing cost and shortening product development cycle.

The mathematical models involving the mass transport of oxygen presented in this review, considered factors such as oxygen diffusivity and solubility of the different materials, initial oxygen concentration in the system, the initial scavenger concentration, as well as the reaction rate and the ratio of moles of scavenger for each mole of oxygen consumed. The time for the oxygen to be consumed or the time for all the scavenger disposed in the system to be used were also observed. Another important factor discussed is the configuration of the multilayer structure, considering cases where the active particles were dispersed throughout the material and/or in layers intercalated with another inert material, as well as the configuration in which they are arranged in multilayer system.

The resolution of the equations that describe the diffusion of oxygen in active polymeric systems from studies reported in this review, was performed by numerical methods, or using specific software. Either way, the solutions found were satisfactory, adequately simulating the performance of oxygen-scavenging particles and active multilayer films. These models can be adapted for other polymers and oxygen scavengers, as well as for the development of other methodologies that describe the oxygen transfer phenomena in active polymeric materials, very promising for future studies.

Funding

This research was funded by Universidade Federal da Fronteira Sul (UFFS) (Edital nº 270/GR/UFFS/2020, PES-2020-0276) and CNPq (grant # 432181/2018-0).

REFERENCES

- Ahn, B. J., Gaikwad, K. K., & Lee, Y. S. (2016). Characterization and properties of LDPE film with gallic-acid-based oxygen scavenging system useful as a functional packaging material. *Journal of Applied Polymer Science*, 133(43), 1–8. <https://doi.org/10.1002/app.44138>
- Akelah, A. (2013). Polymers in Food Packaging Protection. In *Functionalized Polymeric Materials in Agriculture and the Food Industry* (1st ed., pp. 293–347). Springer US. <https://doi.org/10.1007/978-1-4614-7061-8>
- Albis Plastic. (2020). *SELFPLUS O2*. <https://www.albis.com/en/products/products-brands/albis/SHELFPLUS®-O2>
- Andersson, M., Andersson, T., Adlercreutz, P., Nielsen, T., & Hörnsten, E. G. (2002). Toward an enzyme-based oxygen scavenging laminate. Influence of industrial lamination conditions on the performance of glucose oxidase. *Biotechnology and Bioengineering*, 79(1), 37–42. <https://doi.org/10.1002/bit.10266>
- Anukiruthika, T., Sethupathy, P., Wilson, A., Kashampur, K., Moses, J. A., & Anandharamakrishnan, C. (2020). Multilayer packaging: Advances in preparation techniques and emerging food applications. *Comprehensive Reviews in Food Science and Food Safety*, 19, 1156–1186. <https://doi.org/10.1111/1541-4337.12556>
- Apicella, A., Scarfato, P., Di Maio, L., & Incarnato, L. (2018a). Oxygen absorption data of multilayer oxygen scavenger-polyester films with different layouts. *Data in Brief*, 19, 1530–1536. <https://doi.org/10.1016/j.dib.2018.06.024>
- Apicella, A., Scarfato, P., Di Maio, L., & Incarnato, L. (2018b). Transport properties of multilayer active PET films with different layers configuration. *Reactive and Functional Polymers*, 127, 29–37. <https://doi.org/10.1016/j.reactfunctpolym.2018.03.015>
- Ashley, R. J. (1985). Permeability and Plastics Packaging. In J. Comyn (Ed.), *Polymer Permeability* (1nd ed., pp. 269–308). Chapman & Hall. https://doi.org/10.1007/978-94-009-4858-7_7
- Bedane, T., Di Maio, L., Scarfato, P., Incarnato, L., & Marra, F. (2015). Modeling and sensitivity analysis of mass transfer in active multilayer polymeric film for food applications. *AIP Conference Proceedings*, 1695, 020062-1–020062–020068. <https://doi.org/10.1063/1.4937340>
- Belay, Z. A., Caleb, O. J., & Opara, U. L. (2016). Modelling approaches for designing and evaluating the performance of modified atmosphere packaging (MAP) systems for fresh produce: A review. *Food Packaging and Shelf Life*, 10, 1–15. <https://doi.org/10.1016/j.fpsl.2016.08.001>
- Bhunia, K., Sablani, S. S., Tang, J., & Rasco, B. (2013). Migration of chemical compounds from packaging polymers during microwave, conventional heat treatment, and storage. *Comprehensive Reviews in Food Science and Food Safety*, 12(5), 523–545. <https://doi.org/10.1111/1541-4337.12028>
- Bodbodak, S., & Rafiee, Z. (2016). Recent trends in active packaging in fruits and vegetables. In M. W. Siddiqui (Ed.), *Eco-Friendly Technology for Postharvest Produce Quality* (pp. 77–125). Elsevier Inc. <https://doi.org/10.1016/B978-0-12-804313-4.00003-7>
- Brody, A. L., Strupinsky, E. R., & Kline, L. R. (2001). *Active Packaging for Food Applications* (1nd ed.). CRC Press LCC.
- Busolo, M. A., & Lagaron, J. M. (2012). Oxygen scavenging polyolefin nanocomposite films containing an iron modified kaolinite of interest in active food packaging applications. *Innovative Food Science and Emerging Technologies*, 16, 211–217. <https://doi.org/10.1016/j.ifset.2012.06.008>

- Byun, Y., Darby, D., Cooksey, K., Dawson, P., & Whiteside, S. (2011). Development of oxygen scavenging system containing a natural free radical scavenger and a transition metal. *Food Chemistry*, 124(2), 615–619.
<https://doi.org/10.1016/j.foodchem.2010.06.084>
- Callister Jr, W. D. ., & Rethwisch, D. G. (2018). *Materials Science and Engineering: An Introduction* (10th ed.).
- Carranza, S., Paul, D. R., & Bonnecaze, R. T. (2010). Analytic formulae for the design of reactive polymer blend barrier materials. *Journal of Membrane Science*, 360, 1–8. <https://doi.org/10.1016/j.memsci.2010.04.029>
- Carranza, S., Paul, D. R., & Bonnecaze, R. T. (2012). Multilayer reactive barrier materials. *Journal of Membrane Science*, 399–400, 73–85.
<https://doi.org/10.1016/j.memsci.2012.01.030>
- Carrizo, D., Taborda, G., Nerín, C., & Bosetti, O. (2016). Extension of shelf life of two fatty foods using a new antioxidant multilayer packaging containing green tea extract. *Innovative Food Science and Emerging Technologies*, 33, 534–541.
<https://doi.org/10.1016/j.ifset.2015.10.018>
- Clariant Internation Ltd. (2018). *Oxy-Guard™ Oxygen Scavengers*.
<https://www.clariant.com/pt/Solutions/Products/2013/12/09/18/29/OXYGUARD-OXYGEN-SCAVENGERS>
- Cooksey, K. (2010). Oxygen Scavenging Packaging Systems. *Encyclopedia of Polymer Science and Technology*, 1–10. <https://doi.org/10.1002/0471440264.pst570>
- Crank, J., & Park, G. S. (1968). *Diffusion in Polymers* (1nd ed.). Elsevier Science Publishing Co. Inc.
- Crippa, A., Sydenstricker, T. H. D., Amico, S., & C. (2007). Desempenho de filmes multicamadas em embalagens termoformadas. *Polímeros: Ciência e Tecnologia*, 17, 188–193. <https://doi.org/10.1590/s0104-14282007000300006>
- Cruz-Romero, M., & Kerry, J. P. (2016). Packaging systems and materials used for meat products with particular emphasis on the use of oxygen scavenging systems. In E. J. Cummins & J. . Lyng (Eds.), *Emerging Technologies in Meat Processing: Production, Processing and Technology* (1th ed., pp. 231–263). John Wiley & Sons, Ltd. <https://doi.org/10.1002/9781118350676>
- Cruz, R. S., Camilloto, G. P., & Pires, A. C. dos S. (2012). Oxygen Scavengers: An Approach on Food Preservation. In A. A. Eissa (Ed.), *Structure and Function of Food Engineering* (1th ed., Vol. 1, pp. 21–42). InTech.
<https://doi.org/10.5772/48453>
- Dave, P., Chandwani, N., Nema, S. K., & Mukherji, S. (2017). Enhancement in gas diffusion barrier property of polyethylene by plasma deposited SiOx films for food packaging applications. In S. K. Nayak, S. Mohanty, & L. Unnikrishnan (Eds.), *Trends and Applications in Advanced Polymeric Materials* (pp. 255–273). Scrivener Publishing LLC. <https://doi.org/10.1002/9781119364795.ch14>
- Deshwal, G. K., Panjagari, N. R., & Alam, T. (2019). An overview of paper and paper based food packaging materials: health safety and environmental concerns. *Journal of Food Science and Technology*, 56(10), 4391–4403.
<https://doi.org/10.1007/s13197-019-03950-z>
- Dey, A., & Neogi, S. (2019). Oxygen scavengers for food packaging applications: A review. *Trends in Food Science and Technology*, 90, 26–34.
<https://doi.org/10.1016/j.tifs.2019.05.013>
- Di Maio, L., Marra, F., Apicella, A., & Incarnato, L. (2017). Evaluation and modeling of scavenging performances of active multilayer PET based films for food preservation. *Chemical Engineering Transactions*, 57, 1879–1884.

- https://doi.org/10.3303/CET1757314
- Di Maio, L., Marra, F., Bedane, T. F., Incarnato, L., & Saguy, S. (2017). Oxygen transfer in co-extruded multilayer active films for food packaging. *AIChe Journal*, 63(11), 5215–5221. https://doi.org/10.1002/aic.15844
- Dutch Dessicants Company. (2020). *ATCO Oxygen Absorber*.
<https://www.ddc.nl/en/producten/oxygen-absorber/>
- Dvir, I. M., Weizman, O., Lewitus, D., Weintraub, S., Ophir, A., & Dotan, A. (2019). Antimicrobial active packaging combining essential oils mixture: Migration and odor control study. *Polymers for Advanced Technologies*, 30, 2558–2566.
<https://doi.org/10.1002/pat.4642>
- Fang, Z., Zhao, Y., Warner, R. D., & Johnson, S. K. (2017). Active and intelligent packaging in meat industry. *Trends in Food Science and Technology*, 61, 60–71.
<https://doi.org/10.1016/j.tifs.2017.01.002>
- Ferrari, M. C., Carranza, S., Bonnecaze, R. T., Tung, K. K., Freeman, B. D., & Paul, D. R. (2009). Modeling of oxygen scavenging for improved barrier behavior: Blend films. *Journal of Membrane Science*, 329, 183–192.
<https://doi.org/10.1016/j.memsci.2008.12.030>
- Foltynowicz, Z. (2018). Nanoiron-Based Composite Oxygen Scavengers for Food Packaging. In Giuseppe Cirillo, M. A. Kozlowski, & U. G. Spizzirri (Eds.), *Composites Materials for Food Packaging* (1 nd ed., pp. 209–234). Scrivener Publishing LLC. https://doi.org/10.1002/9781119160243.ch6
- Galdi, M. R., & Incarnato, L. (2011). Influence of Composition on Structure and Barrier Properties os Active PET Films for Food Packagind Applications. *Packaging Technology and Science Technology and Science*, 24, 89–102.
<https://doi.org/10.1002/pts.917>
- Galotto, M. J., Guarda, A., & de Dicastillo, C. L. (2015). Antimicrobial Active Polymers in Food Packaging. In G. Cirillo, U. G. Spizzirri, & F. Iemma (Eds.), *Functional Polymers in Food Science* (Vol. 1, pp. 323–353).
<https://doi.org/10.1002/9781119109785.ch10>
- Geueke, B., Groh, K., & Muncke, J. (2018). Food packaging in the circular economy: Overview of chemical safety aspects for commonly used materials. *Journal of Cleaner Production*, 193, 491–505. https://doi.org/10.1016/j.jclepro.2018.05.005
- Gibis, D., & Rieblinger, K. (2011). Oxygen scavenging films for food application. *Procedia Food Science*, 1, 229–234. https://doi.org/10.1016/j.profoo.2011.09.036
- Han, J. W., Ruiz-Garcia, L., Qian, J. P., & Yang, X. T. (2018). Food Packaging: A Comprehensive Review and Future Trends. *Comprehensive Reviews in Food Science and Food Safety*, 17(4), 860–877. https://doi.org/10.1111/1541-4337.12343
- Henkel AG & Co. (2017). *Oxygen Scavenger Compounds for Closures*.
<https://dm.henkel-dam.com/is/content/henkel/brochure-oxygen-savenger-compounds-closures-daraform-celox>
- Hsiao Sung Non-Oxygen Chemical Co. Ltd. (2020). *O-Buster Oxygen Absorber*. 2020-06-10. <https://en.o-buster.com/>
- Hutter, S., Rüegg, N., & Yildirim, S. (2016). Use of palladium based oxygen scavenger to prevent discoloration of ham. *Food Packaging and Shelf Life*, 8, 56–62.
<https://doi.org/10.1016/j.fpsl.2016.02.004>
- Johansson, K., Wineström, S., Johansson, C., Järnström, L., & Jönsson, L. J. (2012). Oxygen-scavenging coatings and films based on lignosulfonates and laccase. *Journal of Biotechnology*, 161(1), 14–18.
<https://doi.org/10.1016/j.jbiotec.2012.06.004>

- Jongberg, S., Wen, J., Tørngren, M. A., & Lund, M. N. (2014). Effect of high-oxygen atmosphere packaging on oxidative stability and sensory quality of two chicken muscles during chill storage. *Food Packaging and Shelf Life*, 1, 38–48. <https://doi.org/10.1016/j.fpsl.2013.10.004>
- Kirwan, M. J., Plant, S., & Strawbridge, J. W. (2011). Plastics in Food Packaging. In R. Coles & M. Kirwan (Eds.), *Food and Beverage Packaging Technology* (2th ed., pp. 157–212). Clackwell Publishing Ltd. <https://doi.org/10.1002/9781444392180>
- Labels, & Labeling. (2003). *Cryovac develops oxygen scavenging labels*. 7 Aug. <https://www.labelsandlabeling.com/news/latest/cryovac-develops-oxygen-scavenging-labels>
- Labuza, T. P., & Breene, W. M. (1989). Applications of “Active Packaging” for Improvement of Shelf-Life and Nutritional Quality of Fresh and Extended Shelf-Life Foods. *Journal of Food Processing and Preservation*, 13, 1–69. <https://doi.org/10.1111/j.1745-4549.1989.tb00090.x>
- Lagarón, J. . (2011). Multifunctional and nanoreinforced polymers for food packaging. In J. . Lagarón (Ed.), *Multifunctional and nanoreinforced polymers for food packaging* (1th ed., p. 693). Woodhead Publishing Ltd. <https://doi.org/10.1017/CBO9781107415324.004>
- Lechevalier, V. (2016). Packaging: Principles and Technology. In R. Jeantet, T. Croguennec, P. Schuck, & G. Brulé (Eds.), *Handbook of Food Science and Technology: Food Process Engineering and Packaging* (1th ed, Vol. 2, pp. 269–315). John Wiley & Sons, Inc. <https://doi.org/10.1002/9781119285229.ch8>
- Lee, J. S., Jeong, S., Lee, H. G., Cho, C. H., & Yoo, S. R. (2018). Development of a Sulfite-Based Oxygen Scavenger and its Application in Kimchi Packaging to Prevent Oxygen-mediated Deterioration of Kimchi Quality. *Journal of Food Science*, 1–10. <https://doi.org/10.1111/1750-3841.14374>
- Lee, S. Y., Lee, S. J., Choi, D. S., & Hur, S. J. (2015). Current topics in active and intelligent food packaging for preservation of fresh foods. *Journal of the Science of Food and Agriculture*, 95, 2799–2810. <https://doi.org/10.1002/jsfa.7218>
- Li, H., Tung, K. K., Paul, D. R., Freeman, B. D., Stewart, M. E., & Jenkins, J. C. (2012). Characterization of oxygen scavenging films based on 1,4-polybutadiene. *Industrial and Engineering Chemistry Research*, 51(21), 7138–7145. <https://doi.org/10.1021/ie201905j>
- Mangaraj, S., Goswami, T. K., & Mahajan, P. V. (2009). Applications of Plastic Films for Modified Atmosphere Packaging of Fruits and Vegetables: A Review. *Food Engineering Reviews*, 1, 133–158. <https://doi.org/10.1007/s12393-009-9007-3>
- Marsh, K., & Bugusu, B. (2007). Food packaging - Roles, materials, and environmental issues: Scientific status summary. *Journal of Food Science*, 72(3), R39–R55. <https://doi.org/10.1111/j.1750-3841.2007.00301.x>
- Mastromatteo, M., & Del Nobile, M. A. (2011). A simple model to predict the oxygen transport properties of multilayer films. *Journal of Food Engineering*, 102(2), 170–176. <https://doi.org/10.1016/j.jfoodeng.2010.08.015>
- Matche, R. S., Sreekumar, R. K., & Raj, B. (2011). Modification of Linear Low-Density Polyethylene Film Using Oxygen Scavengers for Its Application in Storage of Bun and Bread. *Journal of Applied Polymer Science*, 122, 55–63. <https://doi.org/https://doi.org/10.1002/app.33718>
- McKeen, L. W. (2012a). Introduction to Permeation of Plastics and Elastomers. In *Permeability Properties of Plastics and Elastomers* (3th ed, pp. 1–20). Elsevier Inc. <https://doi.org/10.1016/b978-1-4377-3469-0.10001-3>
- McKeen, L. W. (2012b). Introduction to Plastics and Polymers. In *Permeability*

- Properties of Plastics and Elastomers* (3th ed., pp. 21–37). Elsevier Inc.
<https://doi.org/10.1016/b978-1-4377-3469-0.10002-5>
- Mihindukulasuriya, S. D. F., & Lim, L. T. (2014). Nanotechnology development in food packaging: A review. *Trends in Food Science and Technology*, 40, 149–167.
<https://doi.org/10.1016/j.tifs.2014.09.009>
- Mitsubishi Gas Chemical. (2020). *AGELESS Oxygen Absorber*. 2020-06-10.
<https://www.mgc.co.jp/eng/products/sc/ageless/>
- Morris, B. A. (2017). Barrier. In *The Science and Technology of Flexible Packaging* (pp. 259–308). Plastic Design Library. <https://doi.org/10.1016/B978-0-323-24273-8.00008-3>
- Multisorb Filtration Group. (2020). *Oxygen Absorbers*.
<https://www.multisorb.com/oxygen-absorbers/>
- Mumladze, T., Yousef, S., Tatariants, M., Kriukiene, R., Makarevicius, V., Lukošiute, S. I., Bendikiene, R., & Denafas, G. (2018). Sustainable approach to recycling of multilayer flexible packaging using switchable hydrophilicity solvents. *Green Chemistry*, 20(15), 3604–3618. <https://doi.org/10.1039/c8gc01062e>
- PolyOne. (2020). *Oxygen Scavengers*. <https://www.polyone.com/products/polymer-additives/oxygen-scavengers>
- Restuccia, D., Puoci, F., Parisi, O. I., & Picci, N. (2015). Food Applications of Active and Intelligent Packaging: Legal Issues and Safety Concerns. In G. Cirillo, U. G. Spizzirri, & F. Iemma (Eds.), *Functional Polymers in Food Science* (1st ed., Vol. 1, pp. 401–429). S. <https://doi.org/10.1002/9781119109785.ch12>
- Robertson, G. L. (2013). Food Packaging: Principles and Practice, Third Edition. In *Taylor & Francis Group* (Third). CRC Press LCC.
- Robertson, G. L. (2016). Optical, Mechanical and Barrier Properties of Thermoplastic Polymers. In *Food Packaging: Principles and Practice* (3nd ed., pp. 91–130). <https://doi.org/https://doi.org/10.1201/b21347>
- Röcker, B., Rüegg, N., Glöss, A. N., Yeretzian, C., & Yildirim, S. (2016). Inactivation of Palladium-based Oxygen Scavenger System by Volatile Sulfur Compounds Present in the Headspace of Packaged Food. *Packaging and Technology and Science*, 30, 427–442. <https://doi.org/10.1002/pts>
- Rollick, K. L. (2010). *Method of making vapor deposited oxygen-scavenging particles* (Patent No. 2010/0068379 A1).
- Samorì, C., Cespi, D., Blair, P., Galletti, P., Malferrari, D., Passarini, F., Vassura, I., & Tagliavini, E. (2017). Application of switchable hydrophilicity solvents for recycling multilayer packaging materials. *Green Chemistry*, 19(7), 1714–1720. <https://doi.org/10.1039/c6gc03535c>
- Scarfato, P., Avallone, E., Galdi, M. R., Di Maio, L., & Incarnato, L. (2017). Preparation, Characterization, and Oxygen Scavenging of Biodegradable α-Tocoferol/PLA Microparticles for Active Food Packaging Applications. *Polymer Composites*, 38, 1–6. <https://doi.org/https://doi.org/10.1002/pc.23661>
- Schaefer, D., & Cheung, W. M. (2018). Smart Packaging: Opportunities and Challenges. *Procedia CIRP*, 72, 1022–1027. <https://doi.org/10.1016/j.procir.2018.03.240>
- SealedAir. (2020). *Cryovac Freshness Plus Active Barrier*. <https://sealedair.com/food-care/food-care-products/cryovac-freshness-plus-active-barrier>
- Shin, J., & Selke, S. E. M. (2014). Food Packaging. In S. Clark, S. Jung, & B. Lamsal (Eds.), *Food Processing: Principles and Applications* (2nd ed., pp. 249–273). John Wiley & Sons, Ltd. <https://doi.org/10.1002/9781118846315.ch11>
- Silvestre, C., Duraccio, D., & Cimmino, S. (2011). Food packaging based on polymer

- nanomaterials. *Progress in Polymer Science*, 36, 1766–1782.
<https://doi.org/10.1016/j.progpolymsci.2011.02.003>
- Siracusa, V. (2012). Food packaging permeability behaviour: A report. *International Journal of Polymer Science*, 2012, 1–11. <https://doi.org/10.1155/2012/302029>
- Solovyov, S. E., & Goldman, A. Y. (2006a). Optimized design of multilayer barrier films incorporating a reactive layer. I. Methodology of ingress analysis. *Journal of Applied Polymer Science*, 100, 1940–1951. <https://doi.org/10.1002/app.23433>
- Solovyov, S. E., & Goldman, A. Y. (2006b). Optimized design of multilayer barrier films incorporating a reactive layer. II. Solute dynamics in two-layer films. *Journal of Applied Polymer Science*, 100, 1952–1965. <https://doi.org/10.1002/app.23439>
- Solovyov, S. E., & Goldman, A. Y. (2006c). Optimized design of multilayer barrier films incorporating a reactive layer. III. Case analysis and generalized multilayer solutions. *Journal of Applied Polymer Science*, 100, 1966–1977.
<https://doi.org/10.1002/app.23440>
- Summerfield, J. W., Holst, E. J., & Smit, N. R. (2012). *Fresh Meat Color in cavuum packaged or modified atmosphere packaged fresh meat products* (Patent No. US2011/045908).
- Tartakowski, Z. (2010). Recycling of packaging multilayer films: New materials for technical products. *Resources, Conservation and Recycling*, 55(2), 167–170.
<https://doi.org/10.1016/j.resconrec.2010.09.004>
- Tatarants, M., Yousef, S., Sidaraviciute, R., Denafas, G., & Bendikiene, R. (2017). Characterization of waste printed circuit boards recycled using a dissolution approach and ultrasonic treatment at low temperatures. *RSC Advances*, 7(60), 37729–37738. <https://doi.org/10.1039/c7ra07034a>
- Tibbitt, J. M., Cahill, P. J., Rotter, G. E., Sinclair, D. P., Brooks, G. T., & Behrends, R. T. (2007). *Oxygen scavenging monolayer bottles* (Patent No. U.S. 7,214,415 B2).
- Turan, D., Sängerlaub, S., Stramm, C., & Gunes, G. (2017). Gas permeabilities of polyurethane films for fresh produce packaging: Response of O₂ permeability to temperature and relative humidity. *Polymer Testing*, 59, 237–244.
<https://doi.org/10.1016/j.polymertesting.2017.02.007>
- Wani, A. A., Singh, P., & Langowski, H. C. (2014). Food Technologies: Packaging. *Encyclopedia of Food Safety*, 3, 211–218. <https://doi.org/10.1016/B978-0-12-378612-8.00273-0>
- Wineström, S., Johansson, K., Järnström, L., & Jönsson, L. J. (2013). Co-immobilization of oxalate oxidase and catalase in films for scavenging of oxygen or oxalic acid. *Biochemical Engineering Journal*, 72, 96–101.
<https://doi.org/10.1016/j.bej.2013.01.006>
- Wołosiak-Hnat, A., Zych, K., Mężyńska, M., Kifonidis, A., Dajworski, M., Lisiecki, S., & Bartkowiak, A. (2019). LDPE/PET laminated films modified with FeO(OH) × H₂O, Fe₂O₃, and ascorbic acid to develop oxygen scavenging system for food packaging. *Packaging Technology and Science*, 32(9), 457–469.
<https://doi.org/10.1002/pts.2449>
- Wyrwa, J., & Barska, A. (2017). Innovations in the food packaging market: active packaging. *European Food Research and Technology*, 243, 1681–1692.
<https://doi.org/10.1007/s00217-017-2878-2>
- Yildirim, S., Röcker, B., Rüegg, N., & Lohwasser, W. (2015). Development of Palladium-based Oxygen Scavenger: Optimization of Substrate and Palladium Layer Thickness. *Packaging Technology and Science*, 28, 710–718.
<https://doi.org/doi:10.1002/pts.2134>

